



Defense Threat Reduction Agency  
8725 John J. Kingman Road  
MS 6201  
Fort Belvoir, VA 22060-6201



DTRA-TR-13-62

# TECHNICAL REPORT

## Chirped Grating Tunable Lasers for the Infrared Molecular Fingerprint Spectral Region

Approved for public release; distribution is unlimited.

September 2013

HDTRA1-03-D-0009

S.R.J. Brueck

Prepared by:  
University of New Mexico  
OVPR/University Strategic  
MSC02 1660  
1 University of New Mexico  
Albuquerque, NM 87131

**DESTRUCTION NOTICE:**

Destroy this report when it is no longer needed.  
Do not return to sender.

PLEASE NOTIFY THE DEFENSE THREAT REDUCTION  
AGENCY, ATTN: DTRIAC/ J9STT, 8725 JOHN J. KINGMAN ROAD,  
MS-6201, FT BELVOIR, VA 22060-6201, IF YOUR ADDRESS  
IS INCORRECT, IF YOU WISH THAT IT BE DELETED FROM THE  
DISTRIBUTION LIST, OR IF THE ADDRESSEE IS NO  
LONGER EMPLOYED BY YOUR ORGANIZATION.

# REPORT DOCUMENTATION PAGE

Form Approved  
OMB No. 0704-0188

Public reporting burden for this collection of information is estimated to average 1 hour per response, including the time for reviewing instructions, searching existing data sources, gathering and maintaining the data needed, and completing and reviewing this collection of information. Send comments regarding this burden estimate or any other aspect of this collection of information, including suggestions for reducing this burden to Department of Defense, Washington Headquarters Services, Directorate for Information Operations and Reports (0704-0188), 1215 Jefferson Davis Highway, Suite 1204, Arlington, VA 22202-4302. Respondents should be aware that notwithstanding any other provision of law, no person shall be subject to any penalty for failing to comply with a collection of information if it does not display a currently valid OMB control number. **PLEASE DO NOT RETURN YOUR FORM TO THE ABOVE ADDRESS.**

<b>1. REPORT DATE (DD-MM-YYYY)</b> 00-09-2013		<b>2. REPORT TYPE</b> Technical		<b>3. DATES COVERED (From - To)</b> 07/21/2010 - 04/30/2012	
<b>4. TITLE AND SUBTITLE</b> Chirped Grating Tunable Lasers for the Infrared Molecular Fingerprint Spectral Region				<b>5a. CONTRACT NUMBER</b> HDTRA1-03-D-0009	
				<b>5b. GRANT NUMBER</b>	
				<b>5c. PROGRAM ELEMENT NUMBER</b>	
<b>6. AUTHOR(S)</b> S.R.J. Brueck				<b>5d. PROJECT NUMBER</b> 7	
				<b>5e. TASK NUMBER</b> 26	
				<b>5f. WORK UNIT NUMBER</b>	
<b>7. PERFORMING ORGANIZATION NAME(S) AND ADDRESS(ES)</b> University of New Mexico OVPR/University Strategic MSC02 1660 1 University of New Mexico Albuquerque, NM 87131				<b>8. PERFORMING ORGANIZATION REPORT NUMBER</b> OVPR 798B	
<b>9. SPONSORING / MONITORING AGENCY NAME(S) AND ADDRESS(ES)</b> Defense Threat Reduction Agency 8725 John J. Kingman Road Ft. Belvoir, VA 22060 PM/James Reed				<b>10. SPONSOR/MONITOR'S ACRONYM(S)</b> DTRA	
				<b>11. SPONSOR/MONITOR'S REPORT NUMBER(S)</b> DTRA-TR-13-62	
<b>12. DISTRIBUTION / AVAILABILITY STATEMENT</b> Approved for public release; distribution is unlimited.					
<b>13. SUPPLEMENTARY NOTES</b>					
<b>14. ABSTRACT</b> A new approach approach to tunable mid-infrared lasers, an optically pumped, type-II, InGaSb/InAs gain medium with a chirped distributed feedback grating, has been developed. The chirped grating is patterned using an interferometric lithography (IL) technique with spherical wave fronts and etched into the top cladding of the laser slab waveguide structure. A reduced longitudinal chirp grating fabrication technique has been developed that dramatically extends the single frequency tuning range. Continuous tuning of 80nm around 3.1 um with 320 mW single facet output power at 80K and a 1.6nm FWHM is reported. The present device is designed in the 3-to-4 um range which matches a low loss atmospheric transmission window, and covers an important region of molecular vibration spectra, in particular, the hydrocarbon C-H stretch at 3.3 um, making it suitable for atmospheric pressure remote gas sensing of industrially important small molecules such as methane, hydrogen chloride an ammonia.					
<b>15. SUBJECT TERMS</b> fingerprint lasers interferometric lithography waveguide					
<b>16. SECURITY CLASSIFICATION OF:</b>			<b>17. LIMITATION OF ABSTRACT</b>  UU	<b>18. NUMBER OF PAGES</b>	<b>19a. NAME OF RESPONSIBLE PERSON</b> James Reed
<b>a. REPORT</b> Unclassified	<b>b. ABSTRACT</b> Unclassified	<b>c. THIS PAGE</b> Unclassified			<b>19b. TELEPHONE NUMBER (include area code)</b> 703-767-8793

## CONVERSION TABLE

Conversion Factors for U.S. Customary to metric (SI) units of measurement.

MULTIPLY  $\xrightarrow{\hspace{10em}}$  BY  $\xrightarrow{\hspace{10em}}$  TO GET  
 TO GET  $\xleftarrow{\hspace{10em}}$  BY  $\xleftarrow{\hspace{10em}}$  DIVIDE

angstrom	1.000 000 x E -10	meters (m)
atmosphere (normal)	1.013 25 x E +2	kilo pascal (kPa)
bar	1.000 000 x E +2	kilo pascal (kPa)
barn	1.000 000 x E -28	meter <sup>2</sup> (m <sup>2</sup> )
British thermal unit (thermochemical)	1.054 350 x E +3	joule (J)
calorie (thermochemical)	4.184 000	joule (J)
cal (thermochemical/cm <sup>2</sup> )	4.184 000 x E -2	mega joule/m <sup>2</sup> (MJ/m <sup>2</sup> )
curie	3.700 000 x E +1	*giga bacquerel (GBq)
degree (angle)	1.745 329 x E -2	radian (rad)
degree Fahrenheit	$t_k = (t^{\circ}f + 459.67)/1.8$	degree kelvin (K)
electron volt	1.602 19 x E -19	joule (J)
erg	1.000 000 x E -7	joule (J)
erg/second	1.000 000 x E -7	watt (W)
foot	3.048 000 x E -1	meter (m)
foot-pound-force	1.355 818	joule (J)
gallon (U.S. liquid)	3.785 412 x E -3	meter <sup>3</sup> (m <sup>3</sup> )
inch	2.540 000 x E -2	meter (m)
jerk	1.000 000 x E +9	joule (J)
joule/kilogram (J/kg) radiation dose absorbed	1.000 000	Gray (Gy)
kilotons	4.183	terajoules
kip (1000 lbf)	4.448 222 x E +3	newton (N)
kip/inch <sup>2</sup> (ksi)	6.894 757 x E +3	kilo pascal (kPa)
ktap	1.000 000 x E +2	newton-second/m <sup>2</sup> (N-s/m <sup>2</sup> )
micron	1.000 000 x E -6	meter (m)
mil	2.540 000 x E -5	meter (m)
mile (international)	1.609 344 x E +3	meter (m)
ounce	2.834 952 x E -2	kilogram (kg)
pound-force (lbs avoirdupois)	4.448 222	newton (N)
pound-force inch	1.129 848 x E -1	newton-meter (N-m)
pound-force/inch	1.751 268 x E +2	newton/meter (N/m)
pound-force/foot <sup>2</sup>	4.788 026 x E -2	kilo pascal (kPa)
pound-force/inch <sup>2</sup> (psi)	6.894 757	kilo pascal (kPa)
pound-mass (lbm avoirdupois)	4.535 924 x E -1	kilogram (kg)
pound-mass-foot <sup>2</sup> (moment of inertia)	4.214 011 x E -2	kilogram-meter <sup>2</sup> (kg-m <sup>2</sup> )
pound-mass/foot <sup>3</sup>	1.601 846 x E +1	kilogram-meter <sup>3</sup> (kg/m <sup>3</sup> )
rad (radiation dose absorbed)	1.000 000 x E -2	**Gray (Gy)
roentgen	2.579 760 x E -4	coulomb/kilogram (C/kg)
shake	1.000 000 x E -8	second (s)
slug	1.459 390 x E +1	kilogram (kg)
torr (mm Hg, 0 <sup>o</sup> C)	1.333 22 x E -1	kilo pascal (kPa)

\*The bacquerel (Bq) is the SI unit of radioactivity; 1 Bq = 1 event/s.

\*\*The Gray (GY) is the SI unit of absorbed radiation.

## Final Report for the period September 1, 2010 to January 20, 2012

Ref. Contract: DTRA01-03-D-0009-0026 “Chirped Grating Tunable Lasers for the Infrared Molecular Fingerprint Spectral Region”

### Abstract

A new approach to tunable mid-infrared lasers, an optically pumped, type-II, InGaSb/InAs gain medium with a chirped distributed feedback grating, has been developed. The chirped grating is patterned using an interferometric lithography (IL) technique with spherical wave fronts and etched into the top cladding of the laser slab waveguide structure. A reduced longitudinal chirp grating fabrication technique has been developed that dramatically extends the single frequency tuning range. Continuous tuning of 80 nm around 3.1  $\mu\text{m}$  with 320 mW single facet output power at 80K and a 1.6 nm FWHM is reported. The present device is designed in the 3- to 4- $\mu\text{m}$  range which matches a low loss atmospheric transmission window, and covers an important region of molecular vibration spectra, in particular, the hydrocarbon C-H stretch at  $\sim 3.3 \mu\text{m}$ , making it suitable for atmospheric pressure remote gas sensing of industrially important small molecules such as methane, hydrogen chloride and ammonia.

The details of the work on this project are included in the attachments that include a paper to be published in the Proceedings of the SPIE and presentation materials from Photonics West 2012 and CLEO 2012. In addition to these presentations, a provisional patent application has been filed with the US Patent Office on the improved device capabilities developed during this program and on the new approach to low longitudinal chirp grating fabrication.

Highlights by task include:

1. **Task 1.** *Demonstrate lasing in new, tighter confinement structure at 3.1  $\mu\text{m}$  center Wavelength.*
  - New device designed, material grown and tested. Results were improved over previous design.
2. **Task 2.** *Modeling of longitudinally and transversely chirped grating DFB lasers.*
  - Detailed model of chirped grating DFB lasers developed.
  - Successfully explained initially puzzling results on tuning and mode jumps of DFB laser.
  - Demonstrated that longitudinal chirp of the grating was the major issue.
  - New fabrication technique developed to significantly ( $\sim 10\text{X}$ ) reduce chirp and provide better tuning performance.

3. **Task 3.** *Investigate tuning characteristics of DFB lasers with chirped gratings and compare both normal DFB (pump stripe perpendicular to grating) and  $\alpha$ -DFB (pump stripe perpendicular to facets) operation.*

- Achieved continuous tuning of over 80 nm in a DFB configuration. Highest continuous tuning range ever reported. (probably the major result of the program)
- Reduced chirp devices also operated at significantly higher power as a result of the longer effective cavity length. Important for stand-off detection.
- Compared both grating normal and facet normal configurations.

4. **Task 4.** *Iterate tasks 1 and 2 as appropriate as additional experimental and modeling information becomes available.*

- Results captured in highlights for 1-3.

**Task 5.** *Develop laser source at 3.3  $\mu\text{m}$  optimized for hydrocarbon spectroscopy.*

- Material supplied by AFRL as part of program
- Device fabrication with new low-longitudinal chirp design underway.
- Demonstration of  $\text{CH}_4$  spectroscopy (with previous laser designs).
- Combination will provide optimum device structure.

**Task 6.** *Demonstrate molecular absorption spectroscopy (atmospheric pressure).*

- Initial demonstration of  $\text{CH}_4$  spectroscopy.
- New device was at shorter wavelength, no convenient molecular species available.
- Used Fabry-Perot Interferometer as “spectroscopy simulator.”
- Demonstrated high resolution, long wavelength span tuning.
- Developed approach to high speed modulation using high-speed galvanometer to modulate at  $\sim 5$  kHz rates.
- Ultimate sensitivity will be achieved with higher modulation speeds (acousto-optic modulator) to put modulation frequency above laser noise frequencies.

**Task 7.** *Investigate use of multiple heterogeneous quantum wells to extend tuning range.*

- Increased gain bandwidth has been demonstrated in prior work at AFRL.
- Modeling is underway to estimate the available tuning range within the limits of the longitudinal chirp and the device size. Certainly, devices can be provided to cover the entire gain bandwidth.

Attachment A:

**Optically pumped type-II Mid-IR tunable DFB laser**

Xiang He, Steven Benoit, S. R. J. Brueck and R. Kaspi

*Proceedings of SPIE 8277, 82771C (2012)*

# Optically pumped type-II Mid-IR tunable DFB laser

Xiang He<sup>\*a</sup>, R. Kaspi<sup>b</sup> and S. R. J. Brueck<sup>a</sup>

<sup>a</sup>Center for High Technology Materials, University of New Mexico, Albuquerque, NM 87106;

<sup>b</sup>Air Force Research Laboratory, Directed Energy Directorate, Kirtland Air Force Base, Albuquerque, NM 87117

## ABSTRACT

A new approach to tunable mid-infrared lasers, an optically pumped, type-II, InGaSb/InAs gain medium with a chirped distributed feedback grating, has been developed. The chirped grating is patterned using an interferometric lithography (IL) technique with spherical wave fronts and etched into the top cladding of the laser slab waveguide structure. Because the period of grating increases gradually laterally, wavelength tuning is implemented by shifting pump stripe to different positions on the device with different grating periods. Fabry-Perot modes from the cleaved facets are successfully suppressed by fabricating the grating  $6^\circ$  tilted with respect to facets and adjusting the pump stripe normal to the grating. Continuous tuning of 30 nm around  $3.1 \mu\text{m}$  with 320 mW single facet output power at 80K and a 1.6 nm FWHM is reported. The present device is designed in the 3- to  $4\text{-}\mu\text{m}$  range which matches a low loss atmospheric transmission window, and covers an important region of molecular vibration spectra, in particular, the hydrocarbon C-H stretch at  $\sim 3.3 \mu\text{m}$ , making it suitable for atmospheric pressure remote gas sensing of industrially important small molecules such as methane, hydrogen chloride and ammonia.

**Keywords:** Tunable, DFB, Mid-IR, Semiconductor Laser, interferometric lithography, chirped grating,

## 1. INTRODUCTION

Mid-infrared (Mid-IR) semiconductor lasers have achieved significant advances in performance over the past decade. Generally, there are three major types of high performance mid-IR semiconductor-based lasers: electrically pumped intersubband quantum cascade (QC) lasers,<sup>1-4</sup> electrically pumped interband cascade (IC) lasers,<sup>5-9</sup> and optically pumped interband lasers.<sup>11-16</sup> With the exception of the QC lasers, these mid-IR type-II lasers are based on the “W” shaped InAs and InGaSb quantum well structure, first proposed by Meyer *et al.*,<sup>10</sup> shown in Fig. 1a). The “W” shape takes its name from the pattern of the alignment of the different quantum well layers of different materials as shown.<sup>17</sup>

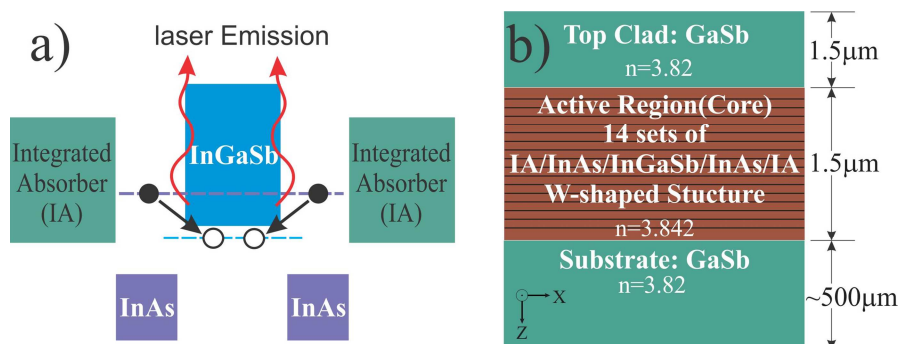


Figure 1. a) Generic epitaxial structure design for optically pumped semiconductor laser. The alignment of the energy bands of the different material layers forms a “W” shaped pattern. The purple and blue dashed lines represent the effective conduction and valence band edges. The solid and open circles stand for electrons and holes respectively. b) Cross section view of the structure of our laser device. In the core layer of the slab waveguide, there are 14 sets of the W-shaped structure shown in a) to fully absorb the pump laser power.

\*xianghe@unm.edu; phone 1 505 272-7920; fax 1 505 272-7801

QC lasers have the advantage of room temperature operation with several hundred mW output power but their output power drops as temperature increases. One of the critical drawbacks of QC lasers is that the efficiency drops rapidly as the output wavelength becomes shorter than  $\sim 4.5 \mu\text{m}$ , making them unsuitable for the important 3- to 5- $\mu\text{m}$  atmospheric window. For the mid-IR range, IC lasers do not achieve high power output with electrical pumping. In comparison, optically pumped type-II IC lasers uniquely provide multi-Watt, continuous-wave, narrow linewidth operation in the important atmospheric transmission window range of 3- to 4.5- $\mu\text{m}$ . They are suitable for applications in remote gas sensing, absorption vibration spectroscopy and mid-IR countermeasures. This paper provides details on a novel approach to an optically pumped, rapidly, widely and continuously tunable, mid-IR DFB laser.

By varying the thickness of the InAs layer, type-II semiconductor lasers cover the range from  $\sim 2.3$ - to 12- $\mu\text{m}$ , including the bulk of the molecular fingerprint spectral region. The laser presented in this paper is an optically pumped type-II tunable DFB laser, operating continuous-wave (CW) with a single longitudinal mode (SLM), a narrow spectral linewidth, high output power, a wide and continuous tuning range and good beam quality. All these features make it a suitable candidate for application to remote sensing for gases such as methane and ammonia in the mid-IR and nerve gases in the LWIR.

Fig. 1b) shows the cross section view of epitaxial structure of the wafer. The slab waveguide structure is grown on a GaSb wafer. In the core of the waveguide, there are 14 sets of integrated absorber-InAs/InGaSb/InAs-integrated absorber structures, evenly distributed across the total thickness of  $1.5 \mu\text{m}$  which is designed so to fully absorb the pump power and allows fundamental transverse mode to lase. The integrated absorber is composed of  $(\text{GaSb})_x(\text{InAs}_{0.89}\text{Sb}_{0.11})_{1-x}$ , lattice matched and band adjusted to uniformly absorb the  $1.908 \mu\text{m}$  pump laser power. The effective refractive index in the core layer is only 0.02 higher than in the clad layers, providing a low confinement factor that has better beam quality and suppresses filaments.<sup>18-19</sup>

## 2. METHODOLOGY

Our approach to achieve a mid-IR tunable DFB laser is novel compared with the traditional tunable lasers based on DFB thermal tunability, external cavities with a grating mirror,<sup>20-23</sup> or Vernier-effect DFB lasers with super structured grating.<sup>24-25</sup> These designs achieve tunability either by changing the temperature and refractive index that requires or by using a frequency selective the grating. Thermal tuning is slow and restricted to small wavelength ranges. External cavity grating approaches require precise alignment and large, heavy vibration isolation approaches.

Our laser is an index-coupled DFB laser which means the grating is only fabricated in the clad layer. In the design of this laser, there are mainly three constraints we need to address: the grating period; the coupling strength; and the transverse mode profile. First, the grating period needs to be within the gain spectrum of the active region, in this case centered at about  $3.06 \mu\text{m}$  at 80 K. By Bragg equation, the grating period should be in the vicinity of the  $419 \text{ nm}$ , given that the effective refractive index is about 3.71.

$$\lambda_{\text{Bragg}} = 2n_{\text{effective}}\Lambda \quad (1)$$

Where  $\lambda_{\text{Bragg}}$  is the Bragg wavelength,  $n_{\text{effective}}$  the modal index and  $\Lambda$  is the grating period. Second, the coupling strength  $\kappa\mathcal{L}$  should be in a range between 1 to 3 to give proper feedback without introduction of spatial hole burning phenomena.

$$\kappa\mathcal{L} = \frac{2|\bar{n}_1 - \bar{n}_2|}{(\bar{n}_1 + \bar{n}_2)\Lambda} \mathcal{L} = \frac{\Delta\bar{n}}{n\Lambda} \mathcal{L} = \frac{2\Delta\bar{n}}{\lambda_{\text{Bragg}}} \mathcal{L} \quad (2)$$

Where  $\kappa$  is the coupling coefficient and  $\bar{n}_{1,2}$  correspond to the effective index of the top or groove segment of the grating in the top clad, and  $\mathcal{L}$  is the cavity length. The equation is for the simple case of a straight grating with 50% duty cycle. For tunability, the grating period  $\Lambda$  is a function of the location on device. Third, the optical confinement of the laser should be above 0.35 but not so high as to compromise the output beam quality and result in filamentation at high pump levels. Using standard DFB laser design rules, the optimum grating depth in the top clad is determined to be 500 nm. Modal index and optical confinement factor in the design of this laser are calculated with online optical simulation software LIGHTS<sup>26</sup> by Dr. Andrew Sarangan at University of Dayton.

Instead of fabricating a uniform grating to select the operational wavelength of laser, we made a quadratically chirped grating using an interferometric lithography (IL) technique by interfering two spherical wavefronts. The experimental setup for IL is shown in Fig. 2. In the Fig. 2a), the collimated 3<sup>rd</sup> harmonic output of a Nd:YAG laser at 355 nm is incident from the left hand side. Half of the beam directly illuminates the plano-convex lens, the other half is reflected from the Lloyd's mirror onto the lens. The lens converts the planar wavefronts to spherical wavefronts that are focused to the two virtual foci A, and B. L is the separation of the two foci and D is their distance to the back surface of the lens, both are incident angle  $\theta$  dependent and graphically solved with Matlab program based on simple ray tracing. To avoid Fabry-Perot (F-P) modes in the laser output, we rotate the die/sample 6° as shown in the figure 2b) to tilt the grating orientation. In this way, when we adjust the pump stripe to be normal to the grating, the F-P modes are successfully suppressed as shown in lasing results.

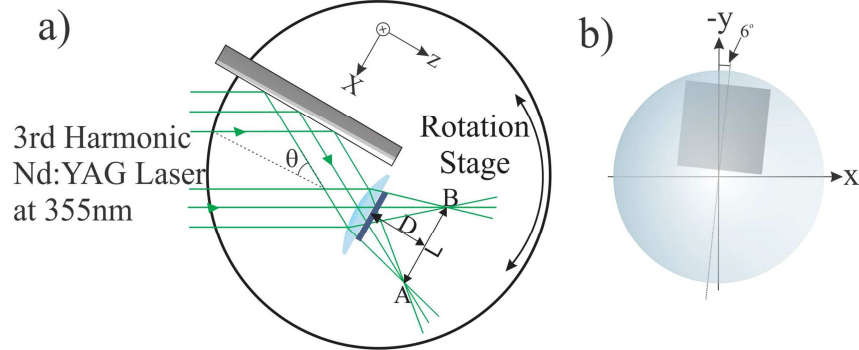


Figure 2 a) Modified Lloyd IL Setup with extra plano-convex lens shown in light blue to convert the planar wave fronts of incident beams to spherical and converges them to two virtual foci A, B behind photoresist coated die shown in dark blue. b) The die is rotated clockwise 6° to make grating tilted with respect to the edge as shown by the grey square.

The grating period on the DFB laser as a function of the coordinates and IL laser wavelength and the location of the two virtual foci is given by the equation:

$$\Lambda(x, y) = \frac{\lambda_{IL}}{\frac{x + L/2}{\sqrt{(x + L/2)^2 + D^2 + y^2}} - \frac{x - L/2}{\sqrt{(x - L/2)^2 + D^2 + y^2}}} \quad (3)$$

Where  $x, y$  are the coordinates on the die. A grating period contour plot including the 6° tilt to the facets is shown in Fig. 3a).

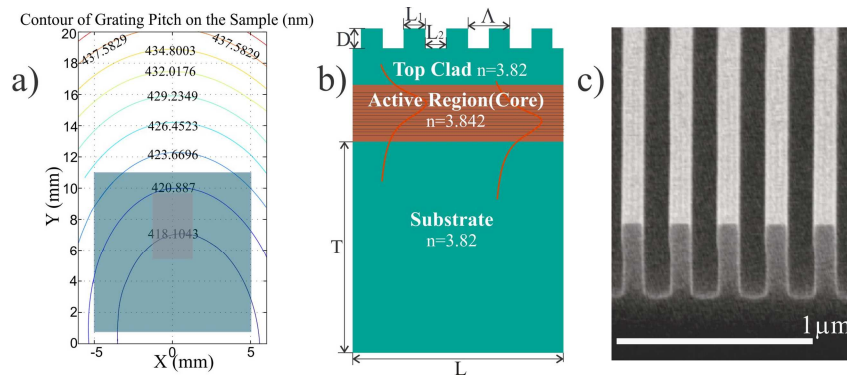


Figure 3. a) Contour plot of the grating pitch as function of location in a 12×20mm zone, for the case of die rotated 6°. The blue square corresponds to the 10×10mm die got from AFRL lab and the grey rectangle represents the 2.5×4 mm<sup>2</sup> DFB device cleaved out from the die. b) Cross section view of the device. Grating period of  $\Lambda \sim 419$  nm is etched into the top clad for  $D = 500$  nm. Substrate is thinned to  $T \sim 150$   $\mu$ m for better thermal conduction. c) SEM picture taken of the grating etched into top clad of device.

Once the grating is patterned in the photoresist, the pattern is transferred into the top of laser's slab waveguide structure shown in Fig. 3b), c) using an inductively coupled plasma (ICP). The grating etch depth into top clad is 500 nm as designed. In figure 3c) shows a SEM picture of the grating after ICP etch. Then the die is thinned down to about 150  $\mu\text{m}$  and a  $4 \times 2.5 \text{ mm}^2$  DFB device is cleaved from the center of the die as shown as the gray rectangle in figure 3a). 4 mm is the lateral dimension of the device, which is picked to give as wide as possible tunable range without cracking issues from non-uniform thermal expansion due to local heating by the pump laser. 2.5 mm is the cavity length picked to give proper coupling strength, also allowing comparison with previously made devices with the same dimension. The final step (Fig. 4a) is indium mounting the device onto a copper heat sink and then to the cold finger of liquid nitrogen Dewar.

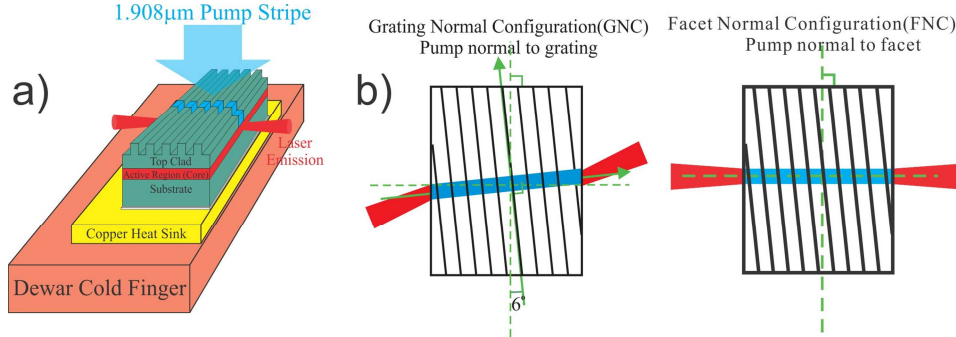


Figure 4. a) Pumping geometry for laser characterization. Device is indium mounted on to a copper heat sink then screwed onto the cold finger of liquid nitrogen Dewar. b) Two different pumping configurations: GNC, pumping normal to the grating; FNC, pumping normal to the facets.

In characterization, a thulium fiber laser at 1.908 nm wavelength is chosen to be the pump laser. Pump stripe is formed with a  $\text{CaF}_2$  cylindrical lens. Benefiting from the flexibility of optical pump, we can rotate the cylindrical lens to adjust the pumping stripe's direction to either perpendicular to the cleaved facets [facet normal configuration (FNC)] or perpendicular to the grating orientation [grating normal configuration (GNC)], as shown in Fig. 4b). The output beam is coupled into a monochromator or Fabry-Perot interferometer together with InSb detector for spectral measurement or into a power meter for output power measurement. Since we have a varying grating period on the device, by shifting the device in lateral direction with pump beam fixed, we pump a different grating period and hence have a different output wavelength.

### 3. RESULTS

Grating normal configuration is the preferred operation configuration, since it successfully suppresses the F-P modes as shown in the plots. All the results shown herein were acquired in GNC. We did operate the laser in FNC for comparison. The device operates in a DFB mode only under a certain pump power, for higher pump power the F-P modes appear in the spectrum and eventually dominate the output spectrum as the pump power is further increased. When the device operates in FNC mode under DFB control, the output wavelength is given by equation (1) with an extra factor of  $\cos(\beta)$ , where  $\beta = 6^\circ$ , corresponds to the titling of the grating orientation with respect to the facets. The other issue of this configuration found in the previously fabricated device is the impact from F-P modes in the composite grating/edge reflector cavity. During wavelength tuning, the spectral peak of the output emission jumps from one F-P mode to the neighboring modes, so the tuning is not continuous. Because of the long cavity length, 2.5  $\mu\text{m}$ , the longitudinal mode spacing is less than a pressure broadened molecular linewidth, so all molecular lines are observed.<sup>16</sup>

All the characterization is at 80K. The device shows about 30 nm of continuous tuning around 3.08  $\mu\text{m}$  as shown in Fig. 5. The device does not lase at both top and bottom edges of the chip, probably due to defects from cleaving. Single facet output power is also measured as function of the pump power. The output power is limited by the available pump power, without any evidence of saturation. Together with Fig. 6, we can conclude that within the whole pump power range, DFB laser operates stably with a single longitudinal mode; the F-P modes are successfully suppressed.

In figure 5a), the blue dots are the experimental data and the red curve is the quadratic fitting of the data to the theoretical expectation of the lasing wavelength from Eq. 3. The experimental data agree with theory fairly well; however, there are a few jumps of the lasing wavelength showing output wavelength changes above or below the theoretical expectation, and sometime device lases on either side of the theoretical value. This is likely due to the degeneracy of DFB modes, and interaction with the longitudinal chirp of the grating, this will be discussed more fully elsewhere. To address this problem, we plan to deposit metal into the grooves of the grating, to introduce asymmetric loss and favor a single longitudinal mode. The waterfall plot in figure 5. shows that across the whole tunable range, the device operates in single longitudinal mode. The F-P modes have been suppressed successfully.

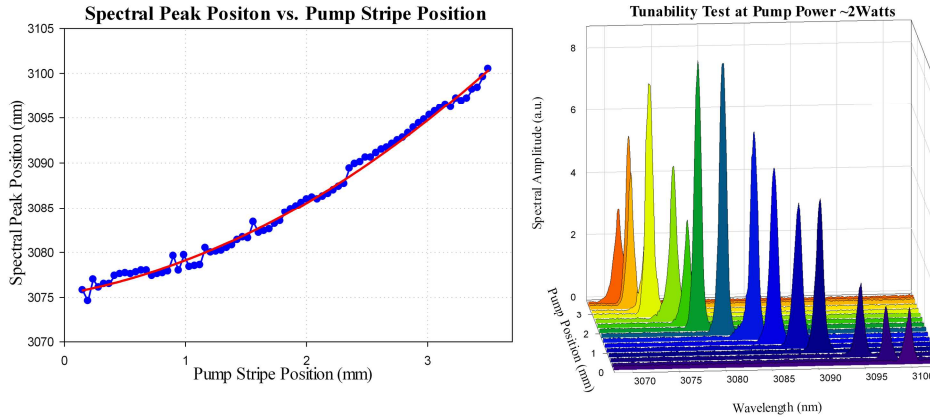


Figure 5. Left: Plot of tunability of the DFB device at 2W pump power, about  $\sim 2X$  threshold. The blue dots are the experimental data and the red curve is the quadratic fitting. Right: Waterfall plot of the spectral at different pump positions, at about  $2X$  threshold of 2W pump powers.

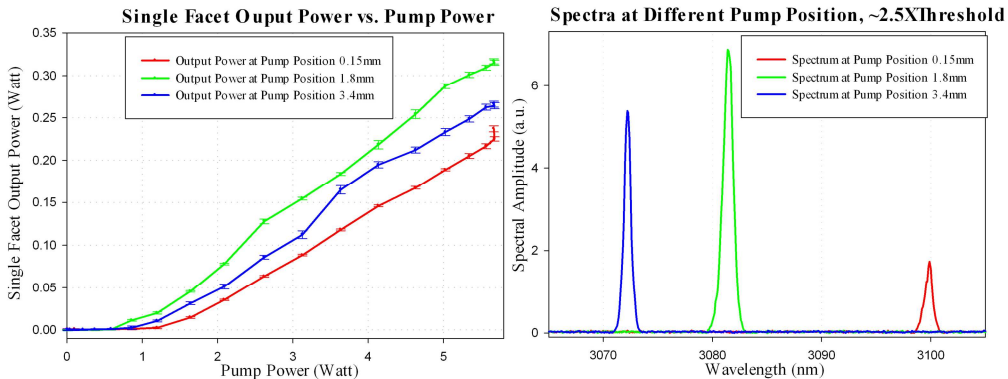


Figure 6. Left: A plot of output power as function of pump power at three different pump stripe positions. Right: Spectra at these three pump positions.

The linewidth of this device is about 1.6 nm at the pump power of about  $2 \times$  threshold. This is large compared with typical low-power, narrow stripe, index guided DFB lasers. The main reasons include: a) the grating patterned with our method varies along the pump stripe as well as transverse to the stripe (the tuning direction). Different grating periods along the stripe will select different lasing wavelength which will broaden the overall line width of the laser output. b) Considering the pump stripe is about  $100 \mu\text{m}$  wide, across it the grating periods varies due to the lateral chirp which broadens the line width of the laser output as well though longitudinal chirp here is dominant reason for wide line width. The longitudinal chirp and lateral chirp are coupled in our approach of the grating patterning and they also depend on the focal length of the plano-convex lens used in IL and the incident angle of the interfering beams. Present value for longitudinal chirp for this device along the pump stripe is about 0.1% which restricts the effective laser length and impacts the line width.

## 4. CONCLUSION

We report a novel technique for the implementation of a mid-IR type-II tunable DFB laser. The present device shows about 30 nm continuous tunable range around 3.1  $\mu\text{m}$  with a single-facet output power of about 320 mW (Fig. 6) and a line width of about 1.6 nm. These characteristics make this laser a suitable candidate for atmospheric pressure spectroscopy. Taking into account the atmospheric transmission windows, this technique is applicable to the remote gas sensing applications for light molecules such as methane, ammonia and hydrogen chloride in 3 to 5  $\mu\text{m}$  range. Extending the dimensions of the device to 10 mm, would give a tunable range on the scale of the laser gain bandwidth of about 200 nm. This would make it possible to resolving multiple spectral lines of multiple target molecules that very convenient for identification of the molecules. Also as mentioned previously, by varying the thickness of InAs layer in this type-II material system, gain spectral could cover in the range from 2 to 12  $\mu\text{m}$ . The technique demonstrated in this paper will be useful for spectroscopy applications from across the entire IR molecular fingerprint region.

## ACKNOWLEDGEMENT

Support for this work was provided by DTRA under contract DTRA01-03-D-0009-0026, by AFOSR, and by and ARO-SBIR grant under subcontract from Southwest Sciences, Santa Fe, NM.

## REFERENCES

- [1] J. Faist, F. Capasso, D. L. Sivcock, C. Sirtori, A. Hutchinson, and A. Y. Cho, "Quantum cascade laser," *Science* **264**, 553-556 (1994).
- [2] A. Evans, J. S. Yu, S. Slivken, and M. Razeghi, "Continuous-wave operation of  $\lambda \sim 4.8 \mu\text{m}$  quantum-cascade lasers at room temperature," *Appl. Phys. Lett.* **85**, 2166-2168 (2004).
- [3] Q. Yang, W. Bronner, C. Manz, R. Moritz, Ch. Mann, G. Kaufel, K. Köhler, and J. Wagner, "Continuous-wave operation of GaInAs-AlGaAsSb quantum cascade lasers," *IEEE Photon. Technol. Lett.* **17**, 2283-2285 (2005)
- [4] Q. Yang, C. Manz, W. Bronner, Ch. Mann, L. Kirste, K. Köhler, and J. Wagner, "GaInAs/AlAsSb quantum cascade lasers operating up to 400 K," *Appl. Phys. Lett.* **86**, 131107 (2005).
- [5] R. Q. Yang, "Mid-infrared interband cascade lasers based on type-II heterostructures," *Microelectron. J.* **30**, 1043-1056 (1999).
- [6] J. L. Bradshaw, J. D. Bruno, J. T. Pham, D. E. Wortman and R. Q. Yang, "Continuous wave operation of type-II interband cascade lasers," *IEEE Proc. Optoelectron.* **147**, 177-180 (2000).
- [7] R. Q. Yang, J. L. Bradshaw, J. D. Bruno, J. T. Pham, and D. E. Wortman, "Mid-infrared type-II interband cascade lasers," *IEEE J. Quant. Electron.* **38**, 559-568 (2002).
- [8] K. Mansour, Y. Qiu, C.J. Hill, A. Soibel and R.Q. Yang, "Mid-infrared interband cascade lasers at thermoelectric cooler temperatures," *Electron. Lett.* **42**, 1034-1035 (2006).
- [9] M. Kim, D. C. Larrabee, J. A. Nolde, C. S. Kim, C. L. Canedy, W. W. Bewley, I. Vurgaftman, and J. R. Meyer, "Narrow ridge interband cascade laser emitting high CW power," *Electron. Lett.* **42**, 1097-1098 (2006).
- [10] J. R. Meyer, C. A. Hoffman, F. J. Bartoli, and L. R. Ram-Mohan, "Type-II quantum-well lasers for the Mid-wave length infrared," *Appl. Phys. Lett.* **67**, 757-759 (1995).
- [11] A. K. Goyal, G. W. Turner, H. K. Choi, P. J. Foti, M. J. Manfra, T. Y. Fan, and A. Sanchez, "High-efficiency optically pumped Mid-IR lasers with integrated absorbers," *Proc. IEEE LEOS* **1**, 249-250 (2000).
- [12] R. Kaspi, A. Ongstad, C. Moeller, and G. C. Dente, "Optically pumped integrated absorber 3.4  $\mu\text{m}$  laser with InAs-to-InGaAsSb type-II transition," *Appl. Phys. Lett.* **79**, 302-304 (2001).
- [13] R. Kaspi, A. Ongstad, G. C. Dente, J. Chavez, M. L. Tilton, and D. Gianardi, "High power and high brightness from an optically pumped InAs/InGaSb type-II Mid-infrared laser with low confinement," *Appl. Phys. Lett.* **81**, 406-408 (2002).
- [14] R. Kaspi, A. P. Ongstad, G. C. Dente, J. R. Chavez, M. L. Tilton, and D. M. Gianardi, "High performance optically pumped antimonide lasers operating in the 2.4-9.3  $\mu\text{m}$  wavelength range," *Appl. Phys. Lett.* **88**, 041122 (2006).
- [15] Liang Xue, S.R. J. Brueck and R. Kaspi, "High-power continuous-wave single-longitudinal-mode operation of an optically pumped DFB laser at  $\lambda \sim 3.64 \mu\text{m}$ ," *Photon. Tech. Lett.* **20**, 727 (2008).

- [16] Liang Xue, S. R. J. Brueck and R. Kaspi, "Widely tunable distributed-feedback lasers with chirped gratings," *Appl. Phys. Lett.* **94**, 161102 (2009).
- [17] A. Krier (Ed.), [Mid-infrared Semiconductor Optoelectronics], Springer-Verlag London Limited, 189-218 (2006)
- [18] G. C. Dente, "Low confinement factors for suppressed filaments in semiconductor lasers," *IEEE J. Quant. Electron.* **37**, 1650-1653 (2001).
- [19] R. Kaspi, A. Ongstad, G. C. Dente, J. Chavez, M. L. Tilton, and D. Gianardi, "High power and high brightness from an optically pumped InAs/InGaSb type-II Mid-infrared laser with low confinement," *Appl. Phys. Lett.* **81**, 406-408 (2002).
- [20] M. Ito and T. Kimura, "Oscillation properties of AlGaAs DH Lasers with an external grating," *IEEE J. Quant. Electron.* **QE-16**, 69-77 (1980).
- [21] R. Wyatt, W. J. Devlin, "10 kHz Linewidth 1.5 mm InGaAsP External cavity laser with 55 nm tuning Range," *Electron. Lett.* **19**, 110-112 (1983).
- [22] B. Glance, C. A. Burrus, and L. W. Stulz, "Fast frequency-tunable external-cavity laser," *Electron. Lett.* **23**, 98-100 (1987).
- [23] Y. Hori, H. Asakura, F. Sogawa, M. Kato, and H. Serizawa, "External-cavity semiconductor laser with focusing grating mirror," *IEEE J. Quant. Electron.* **26**, 1747-1755 (1990).
- [24] Todt, R., Jacke, T., Meyer, R., Adler, J., Laroy, R., Morthier, G., Amann, M.-C., "Sampled grating tunable twin-guide laser diodes with over 40-nm electronic tuning range," *IEEE Photon. Technol. Lett.* **17**, 2514-2516 (2005).
- [25] Jens, Buus, Markus-Christian Amann, Daniel J. Blumenthal, [Tunable Laser Diodes and Related Optical Sources] 2<sup>nd</sup> Edition, Wiley-IEEE Press, 169-211 (2005).
- [26] [www.nano-fab.com/lights/](http://www.nano-fab.com/lights/).

Attachment B:

**Optically pumped type-II Mid-IR tunable DFB laser**

Xiang He, Steven Benoit, S. R. J. Brueck and R. Kaspi  
Photonics West, 2012

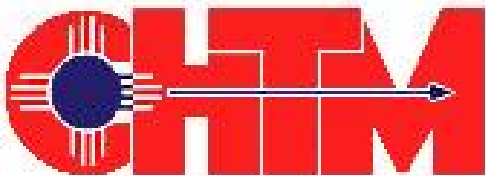
Presentation materials

# Optically Pumped Type-II Mid-IR Tunable DFB Laser

Xiang He<sup>a</sup>, R. Kaspi<sup>b</sup> and S. R. J. Brueck<sup>a</sup>

<sup>a</sup>Center for High Technology Materials, University of New Mexico,  
Albuquerque, NM 87106

<sup>b</sup>Air Force Research Laboratory, Directed Energy Directorate,  
Kirtland Air Force Base, Albuquerque, NM 87117



# Outline

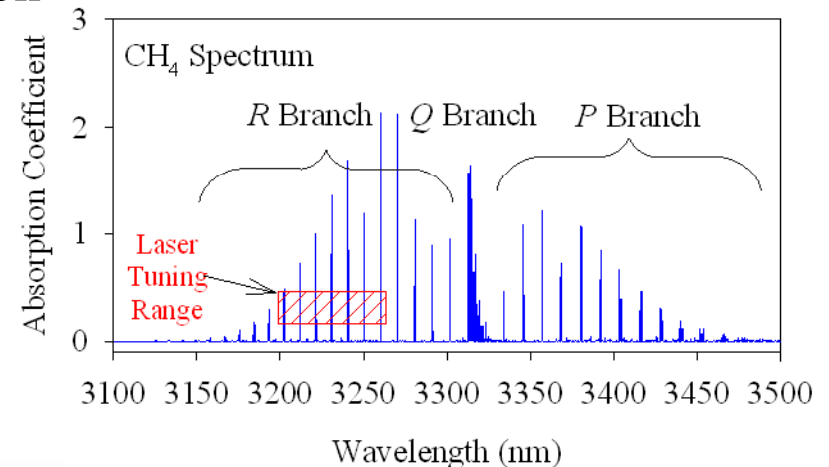
- Applications of Mid-IR Lasers
- Introduction to GaSb Type-II Mid-IR OPSL
- Our approach to achieve tunable DFB laser
- Preliminary experimental results
- Summary
- Future work

# Applications of Mid-IR Lasers

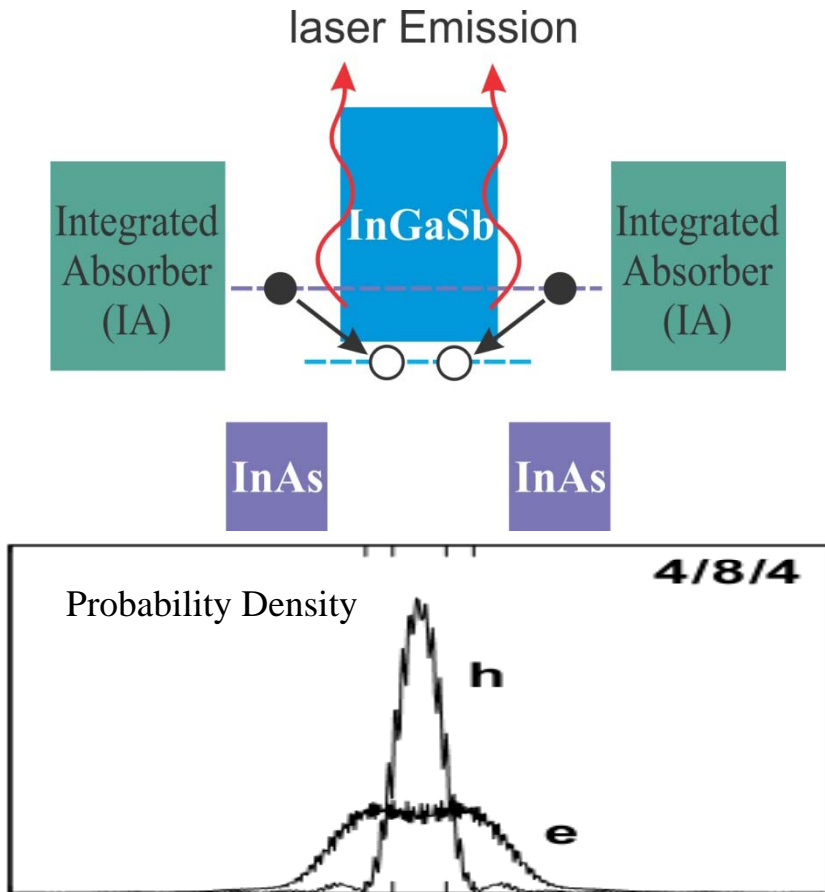
- Spectroscopic sensing/monitoring of substances
- Tunable Laser Diode Absorption Spectroscopy (TLDas)
  - Remote chemical/trace gases sensing:  $\text{CH}_4$ ,  $\text{HCl}$ ,  $\text{NH}_3$ ,  $\text{CO}$ ,  $\text{NO}$ ,  $\text{NO}_2$ ...
  - Atmospheric pollution monitoring/leak detection
  - Chemical process control
  - Defense application: nerve gas detection

- IR illumination and range finder

- Infrared countermeasures



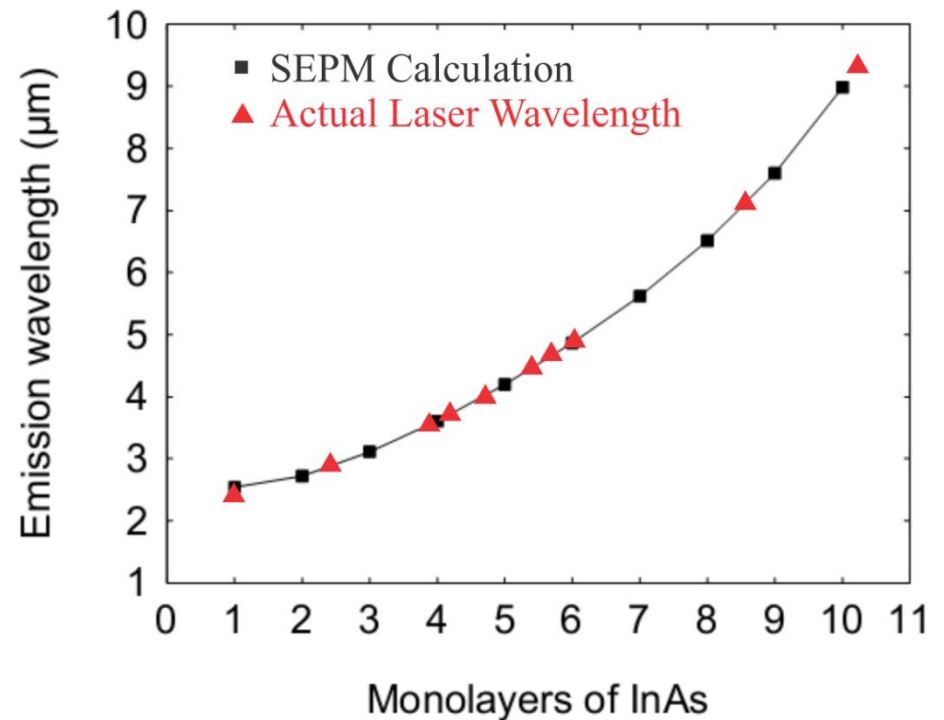
# Introduction to GaSb Type-II Mid-IR OPSL



Meyer et al., APL 67, 1995

Goyal et al., Proc. LEOS 2000

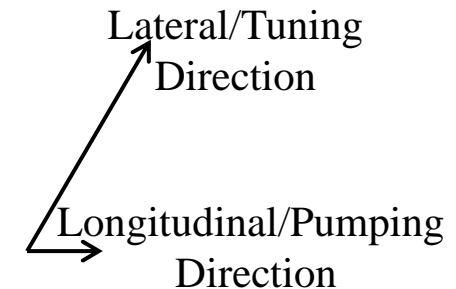
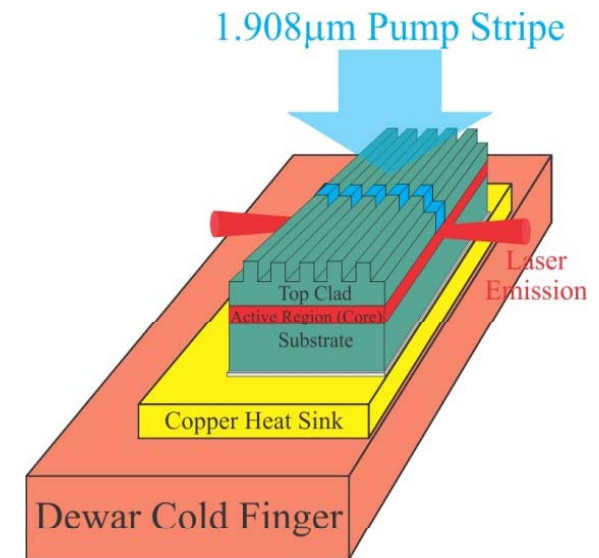
Lasers span 2.3 – 9.5  $\mu\text{m}$  wavelengths



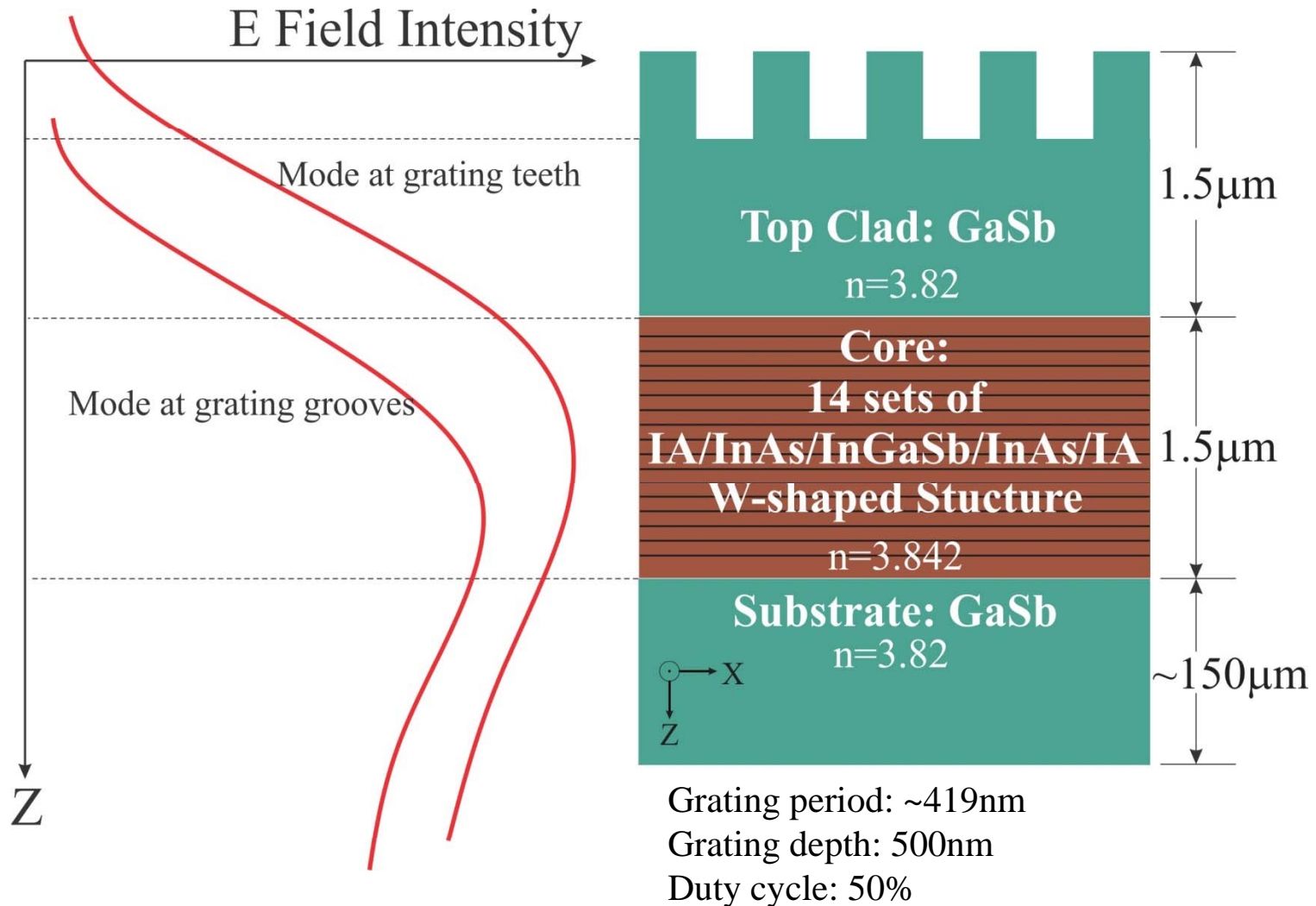
*Kaspi et al.*, Mid-infrared Semiconductor Optoelectronics, Springer

# Our Approach to Tunable DFB Laser

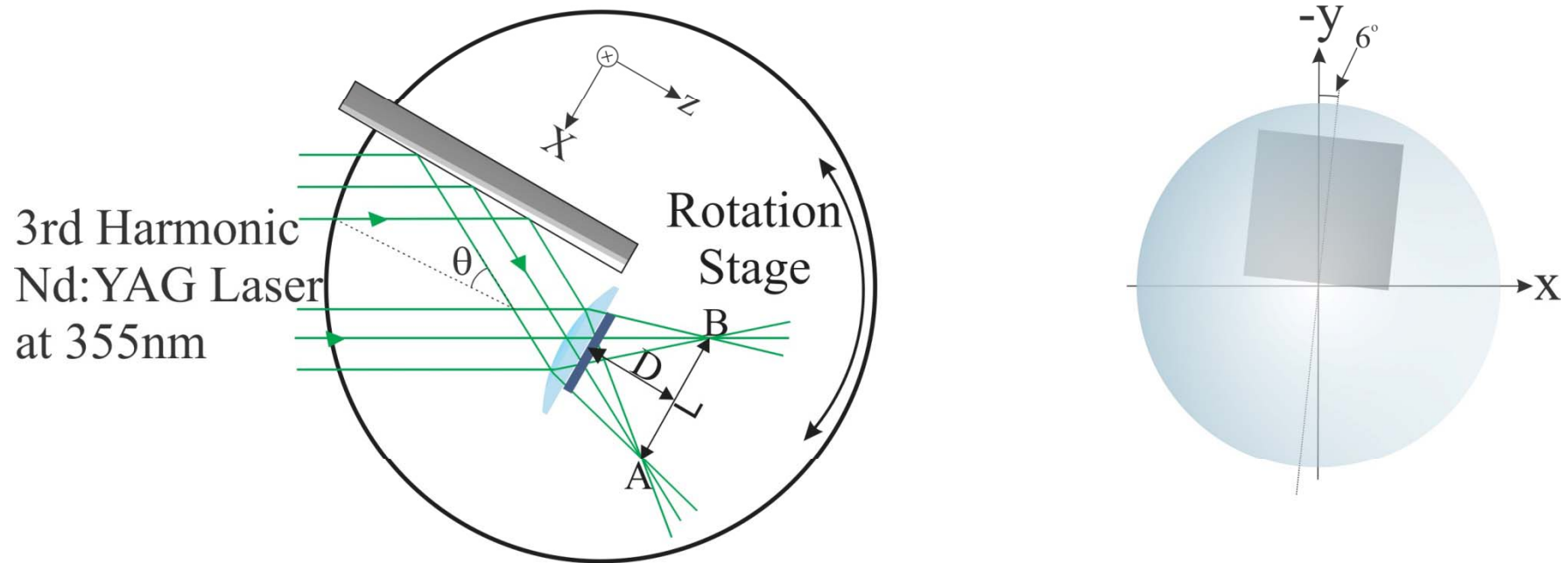
- Chirped grating in top clad of the slab waveguide structure- Index coupled DFB laser
- Optically pumped, with flexibility of varying pumping angle/lateral position- gain guided in lateral direction
- Laterally shift pumping stripe at different positions; grating of different periods select different lasing wavelengths to achieve tuning.



# Slab Waveguide Structure and Mode Distribution



# Interferometric Lithography Setup For Chirped Grating Fabrication

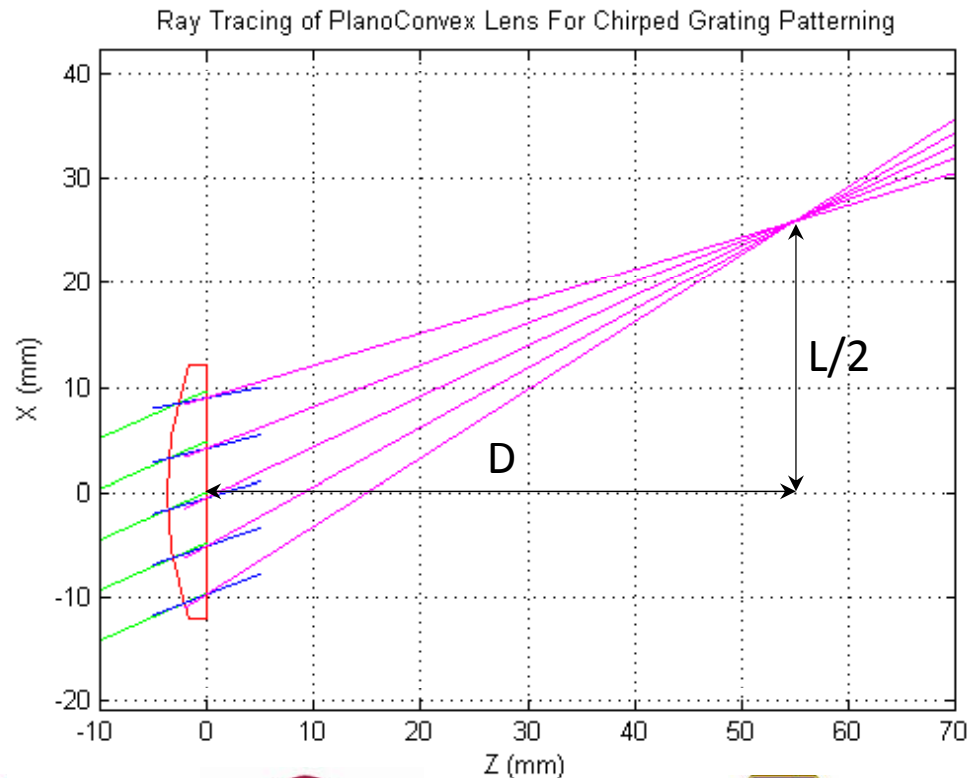


- 5% lateral chirp was obtained in 10-mm wide device.
- Large area ( $20 \times 20 \text{ mm}^2$ ) can be done by IL.
- Grating period and chirp adjustable by changing lens and/or incidence angle.

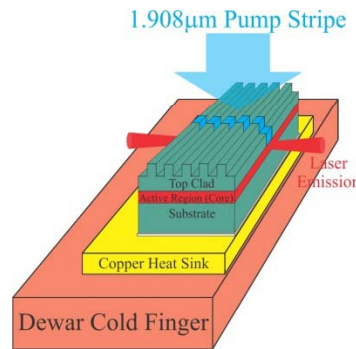
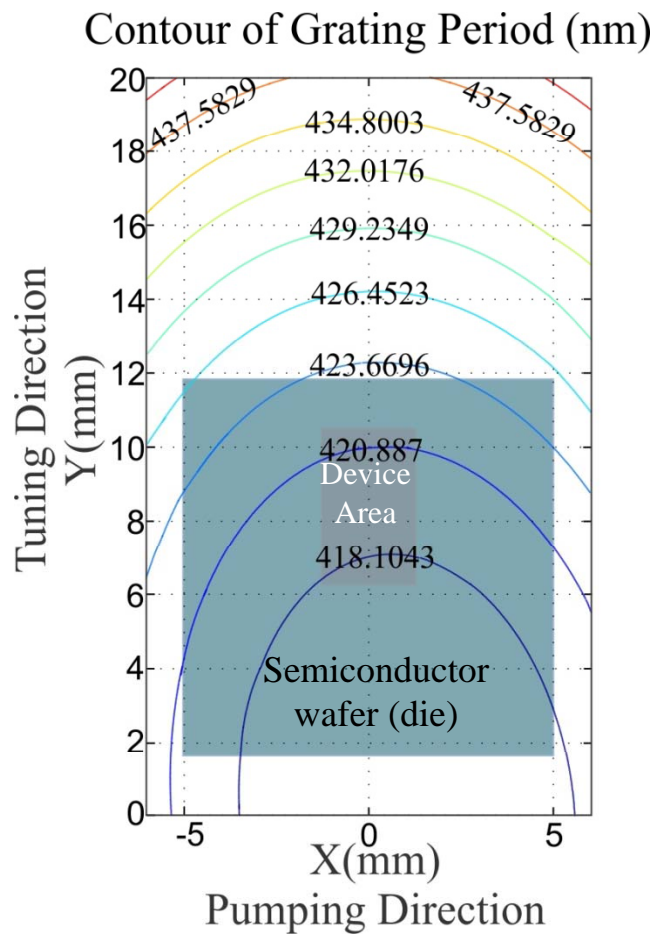
# Chirped Grating Period Calculation

**Grating period:**  $\Lambda(x, y) = \frac{\lambda_{IL}}{\frac{x + L/2}{\sqrt{(x + L/2)^2 + D^2 + y^2}} - \frac{x - L/2}{\sqrt{(x - L/2)^2 + D^2 + y^2}}}$

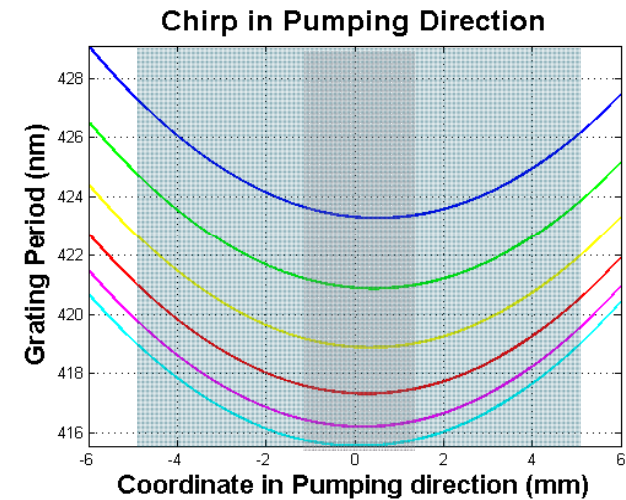
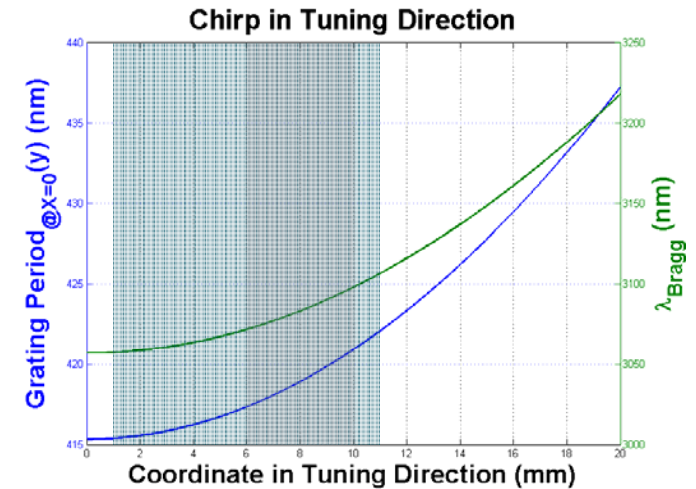
Virtual Foci Locations  
calculated graphically  
using Matlab.



# Chirp of Grating

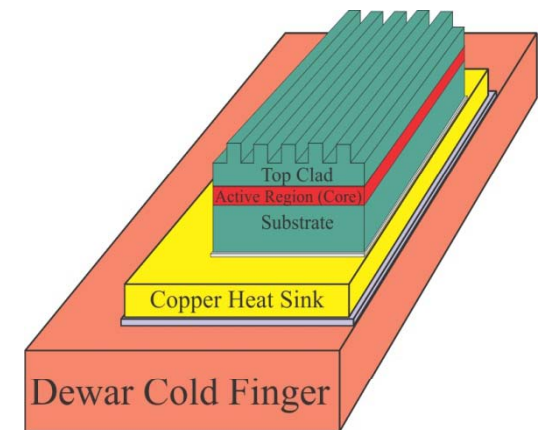
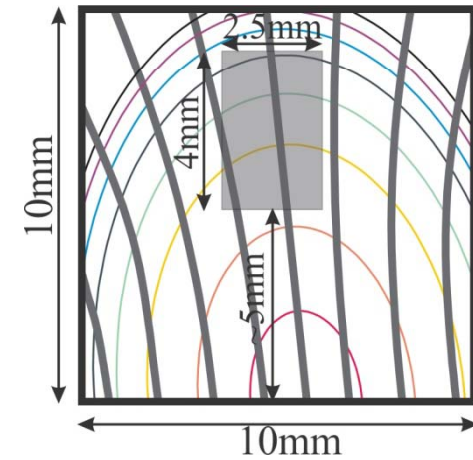
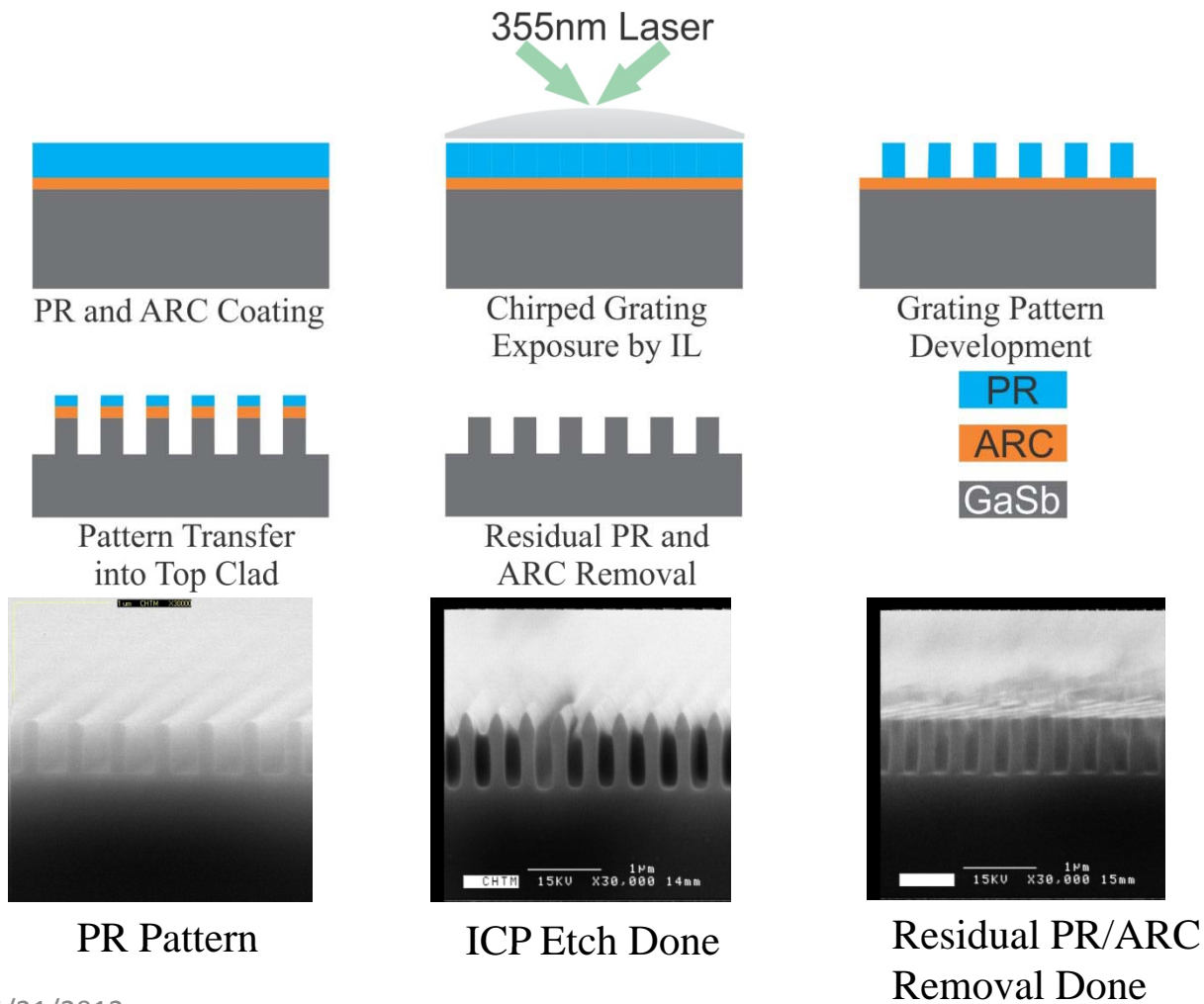


**4×2.5mm Device**  
 Grating Period:  
**[417.39, 421.05]nm**  
 Lateral Chirp:  
**0.87%**  
 Longitudinal Chirp:  
**0.059%-0.099%**

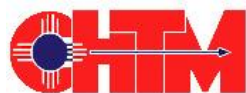


Hyperbolically Chirped Grating

# Fabrication

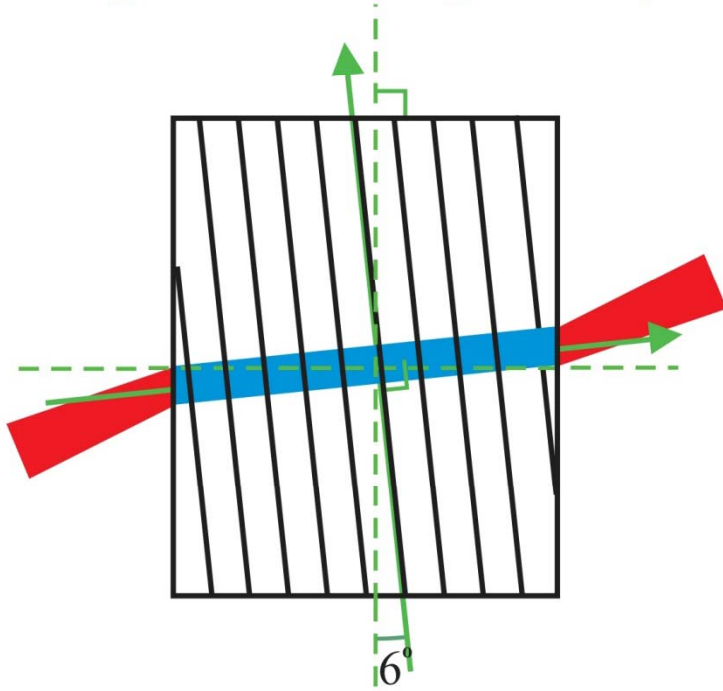


5/21/2012



# Pumping Geometry

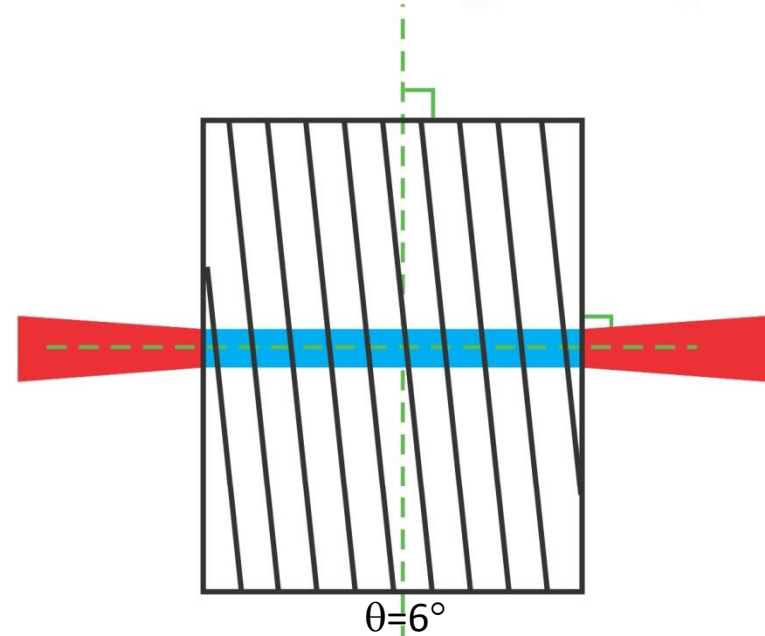
## Grating Normal Configuration(GNC)



$$\lambda_{DFB} = 2n_{eff}\Lambda_{grating}$$

Preferred because of efficient suppression of F-P modes from facet reflection.

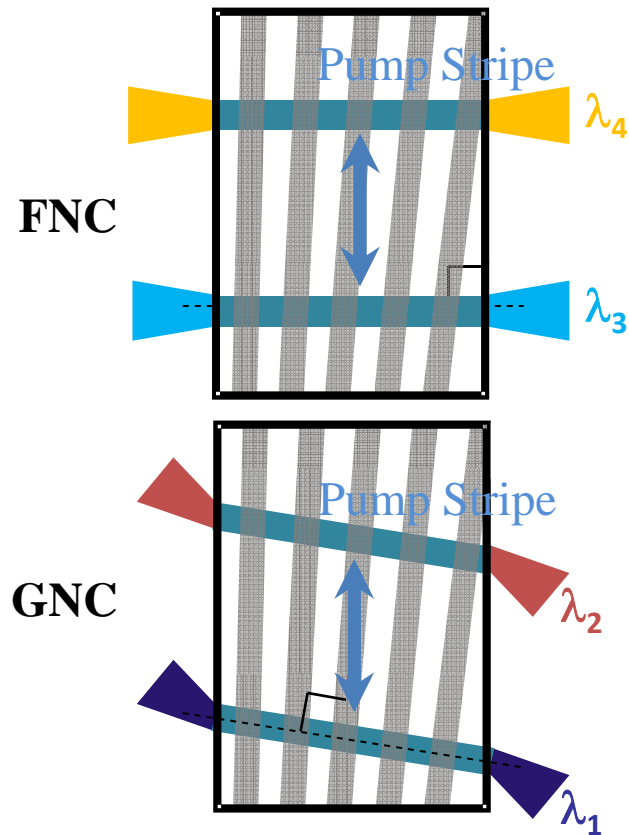
## Facet Normal Configuration(FNC)



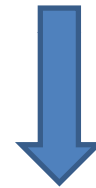
$$\lambda_{\alpha DFB} = 2n_{eff}\Lambda_{grating} \cos(\theta)$$

Take advantage of facet reflection  
Single F-P mode operation at fairly low pump power.

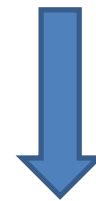
# Tunability Implementation



Shift Pump at Different Positions,  
with Different Angles

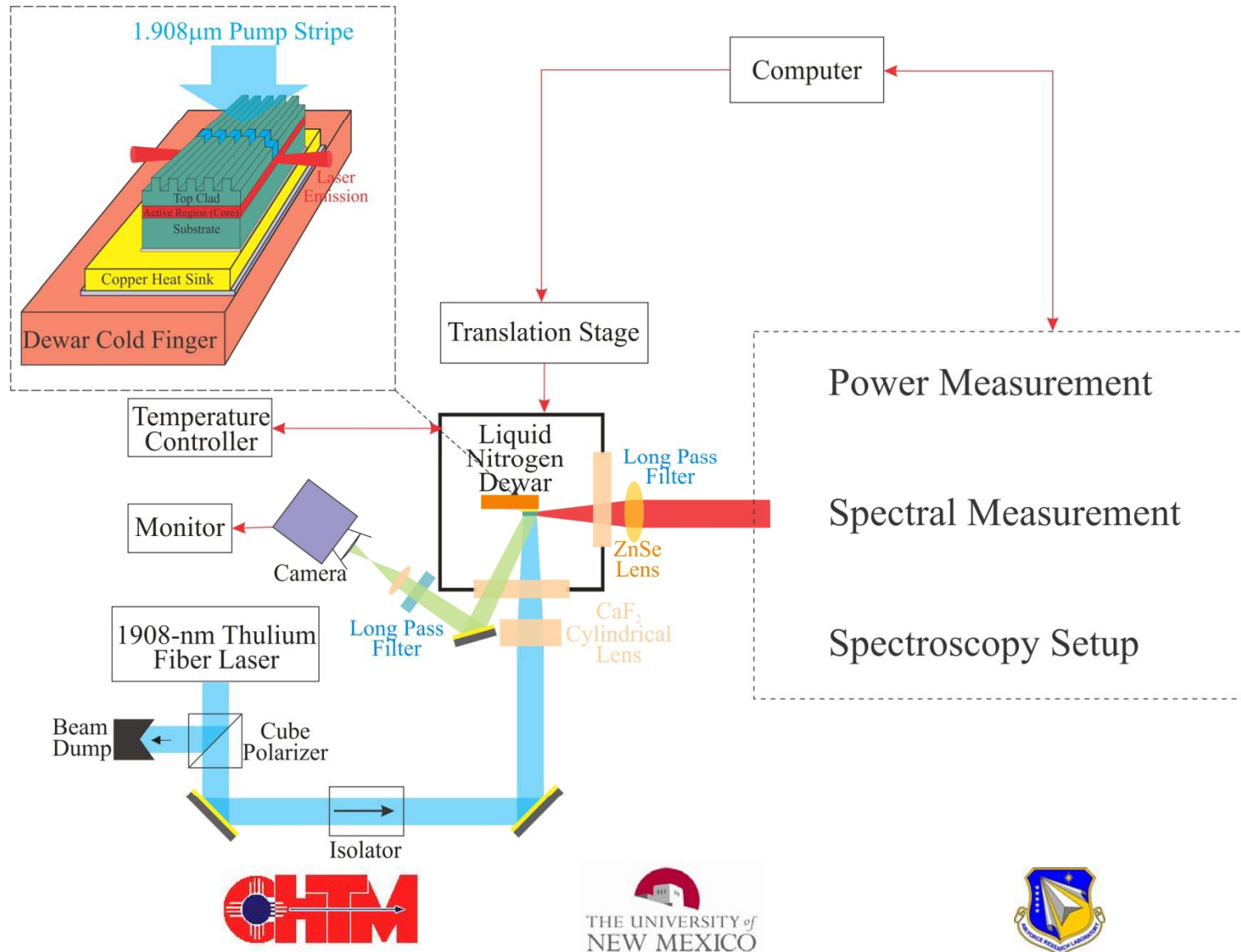


Feedback from Grating of Different Periods

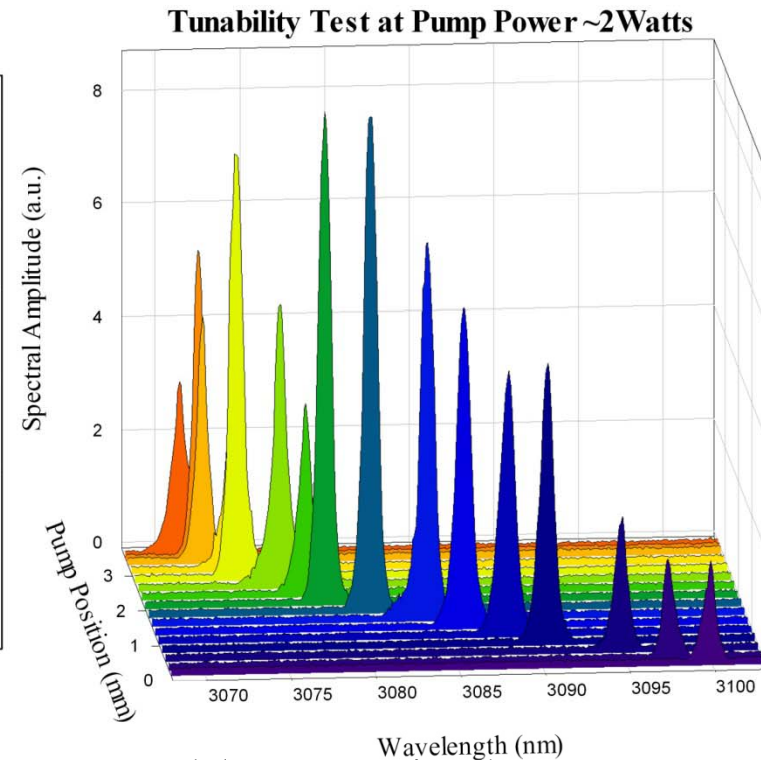
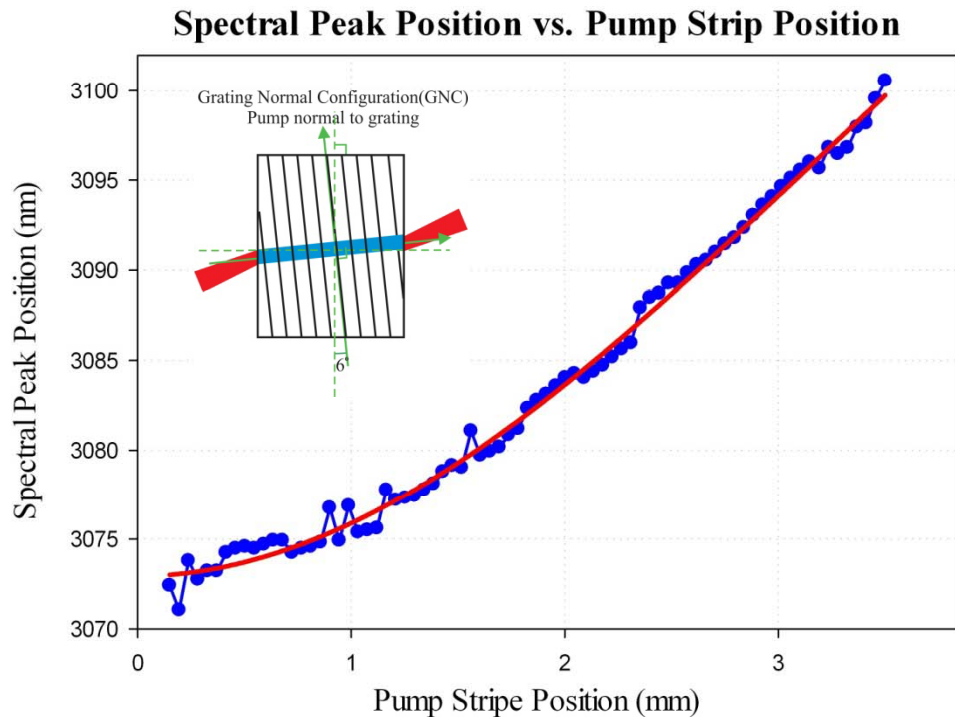


Tunable Wavelengths

# Experimental Setup

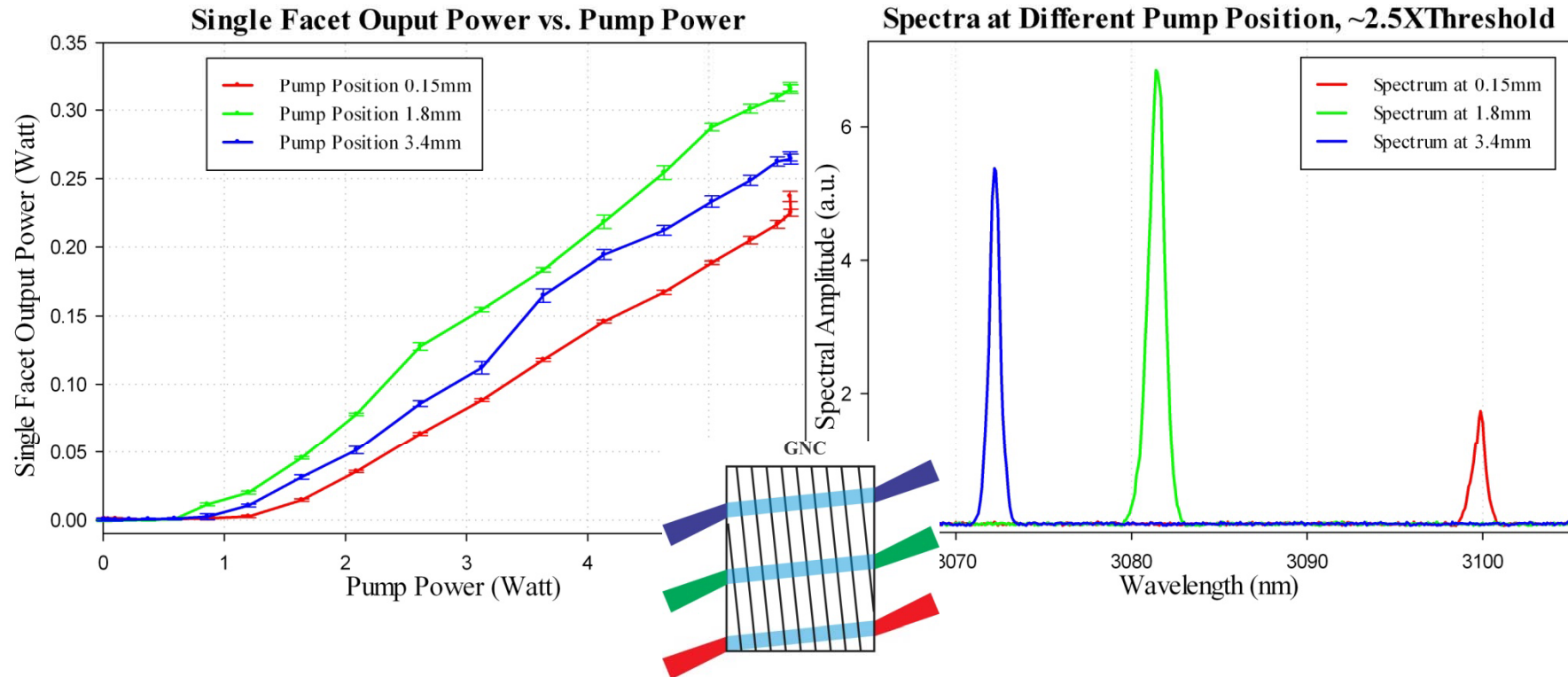


# Tunability Measurement Results



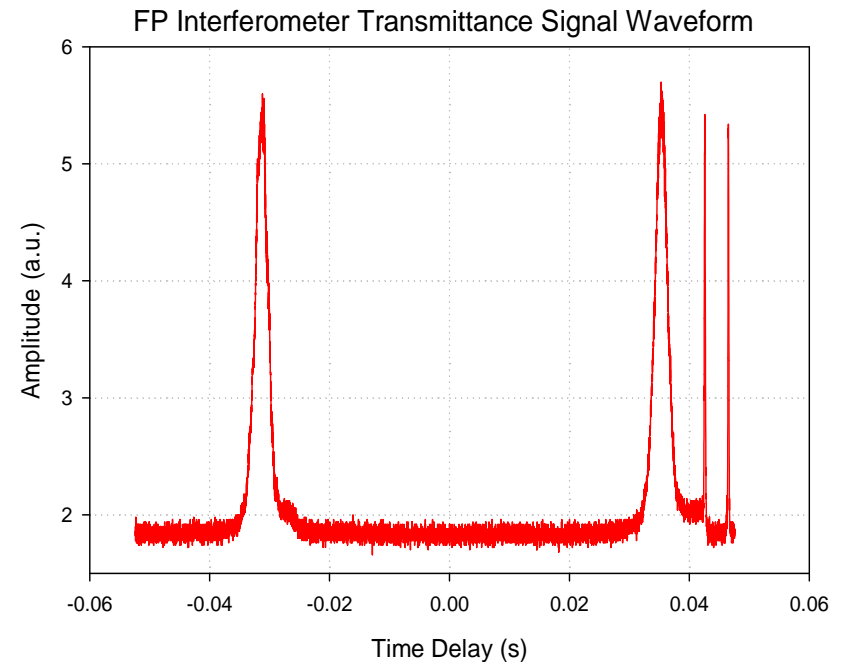
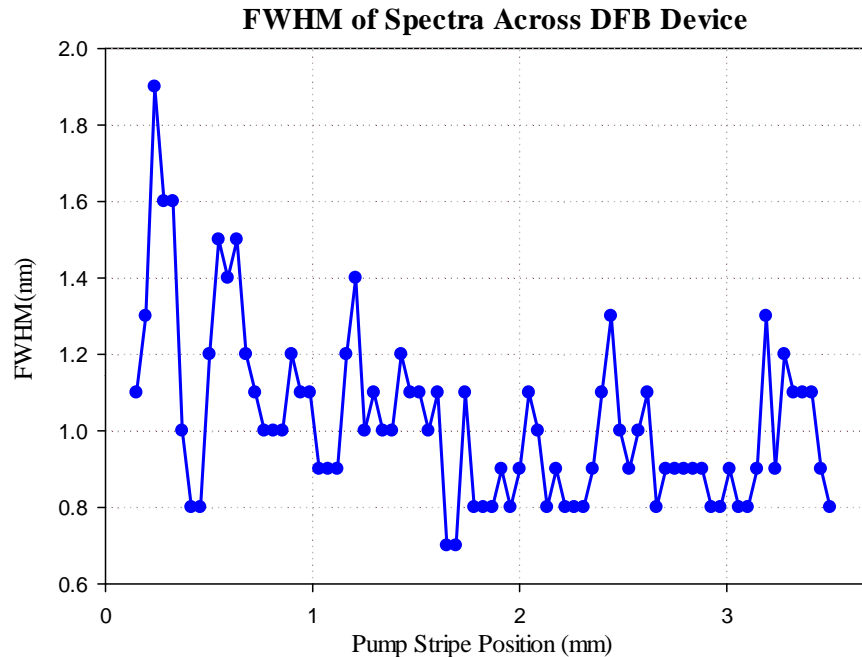
- Tunable range of about 30-nm, continuous tunable range is shorter
- Mode hopping due to longitudinal chirp and DFB mode degeneracy
- Single mode (DFB mode) operation across the whole tunable range

# Output Power Measurement



- Achieved over 320mW single facet output power
- Output power limited by available pump, no roll over
- Single mode (DFB mode) operation across the whole pump power range

# Spectral Linewidth Measurement



F-P interferometer Cavity length  $L \sim 500 \mu\text{m}$ .

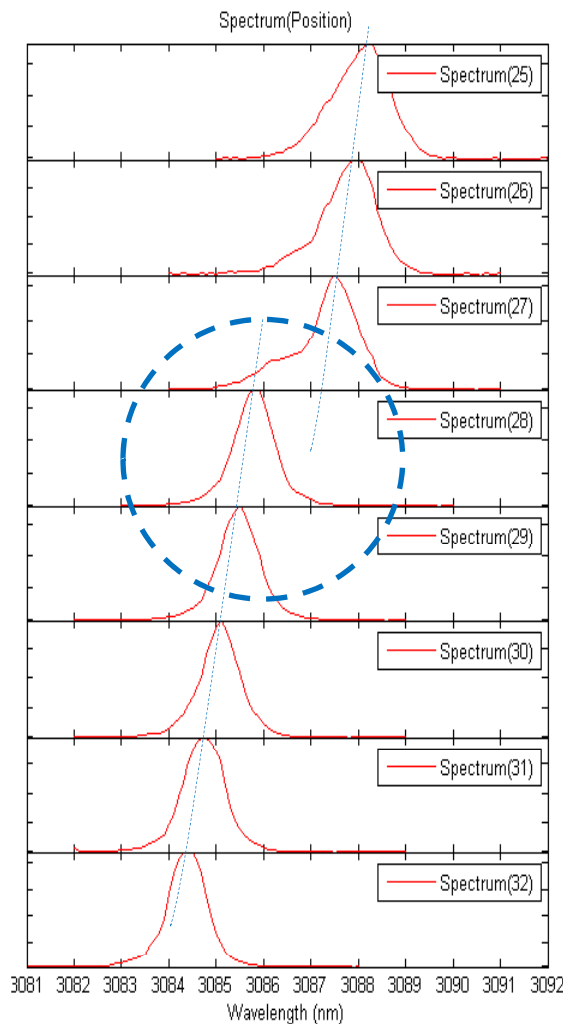
Get wavelength information using monochromator

- Typical linewidth:  $1.2 \text{ nm} @ \sim 2 \times \text{Threshold}$
- Confirmed by monochromator and F-P interferometer
- Structure in spectra at some pump positions due to longitudinal chirp and DFB mode degeneracy

$$FSR = \frac{C}{2nL}$$

$$\Delta\lambda = \frac{\lambda^2}{C} \Delta\nu$$

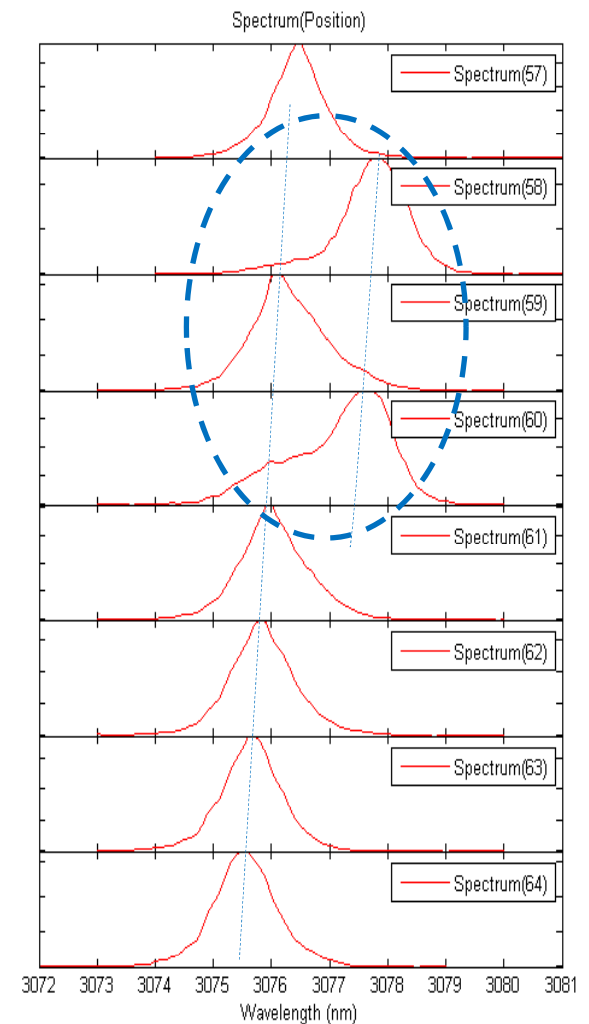
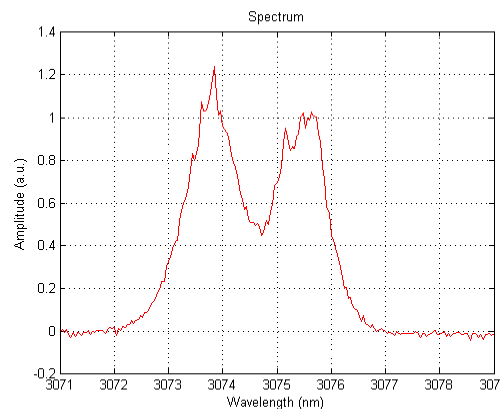
# Longitudinal Mode Hopping Through Chirped DFB Reflectivity Peaks



$$\Delta\lambda = \frac{\kappa\lambda^2}{\pi}$$

$\kappa L \approx 1.4$

Significantly smaller than straight grating calculated values, due to longitudinal chirp and short effective cavity length.



# Summary

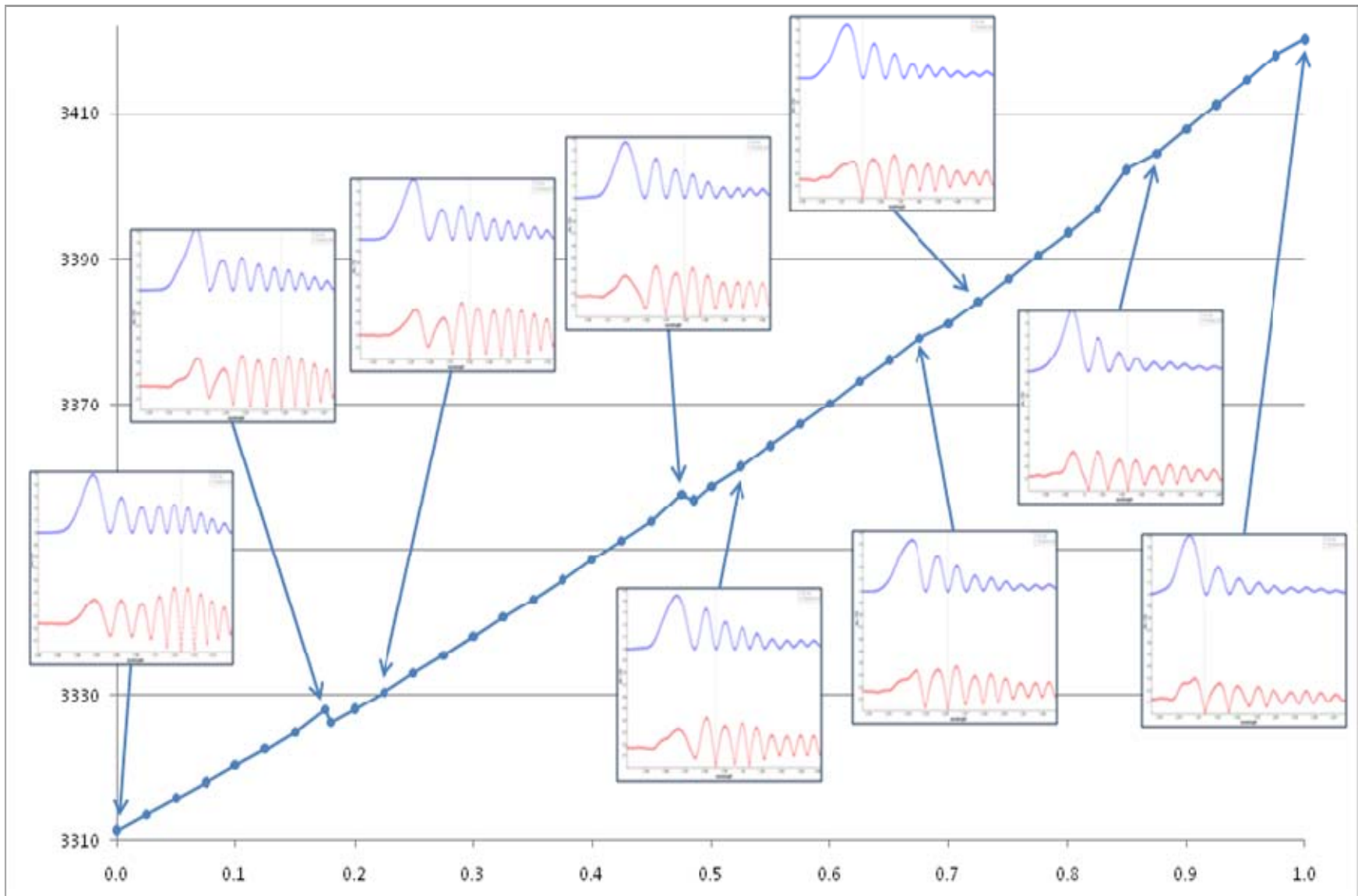
- CW single longitudinal mode operation with tunable range of 30nm (with mode hopping)
- Single facet output power of 320mW @ 80K, limited by available pump
- Typical spectral linewidth of 1.2nm
- Optically pumped type-II tunable DFB laser could be an excellent high-power widely-tunable single-longitudinal-mode light source for atmospheric pressure spectroscopic applications.
- Novel wavelength tuning method, could be applied to different types of lasers.

# Future Work

- Eliminate DFB mode jumps using gain/loss coupling
- Reduce longitudinal chirp
  - e-beam lithography
  - Revised optical lithography arrangement
- Broaden the tunable range by optimizing the focal length of plano-convex lens and incidence angle
- Gas absorption spectroscopy demonstration

**Thank You !  
And  
Questions?**





Based on Simulation by Steve Benoit

Attachment C

**Optically Pumped Type-II Mid-IR Tunable DFB Laser**

Xiang He, Steven J. Benoit, S. R. J. Brueck and R. Kaspi

CLEO 2012

Presentation materials

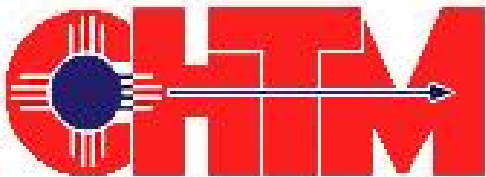
# Optically Pumped Type-II Mid-IR Tunable DFB Laser

Xiang He<sup>a</sup>, Steve Benoit<sup>b</sup>, R. Kaspi<sup>c</sup> and S. R. J. Brueck<sup>a</sup>

<sup>a</sup>Center for High Technology Materials, University of New Mexico, Albuquerque,  
NM 87106

<sup>b</sup> Department of Mathematics, Colorado State University, Fort Collins , CO 80523

<sup>c</sup>Air Force Research Laboratory, Directed Energy Directorate,  
Kirtland Air Force Base, Albuquerque, NM 87117

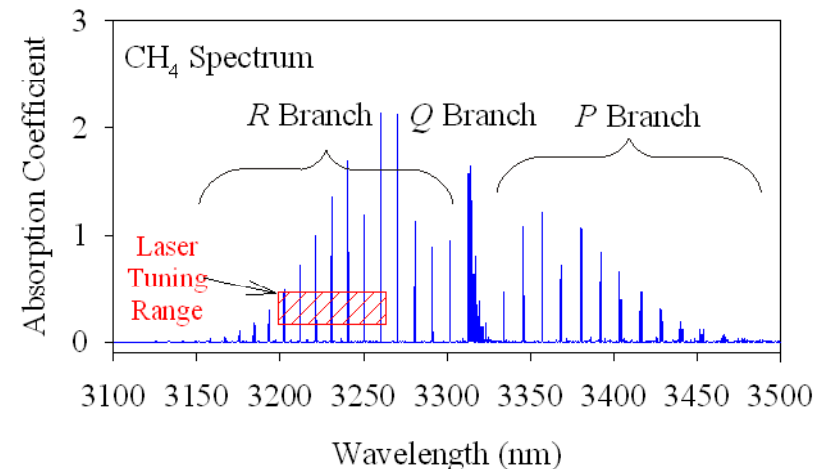


# Outline

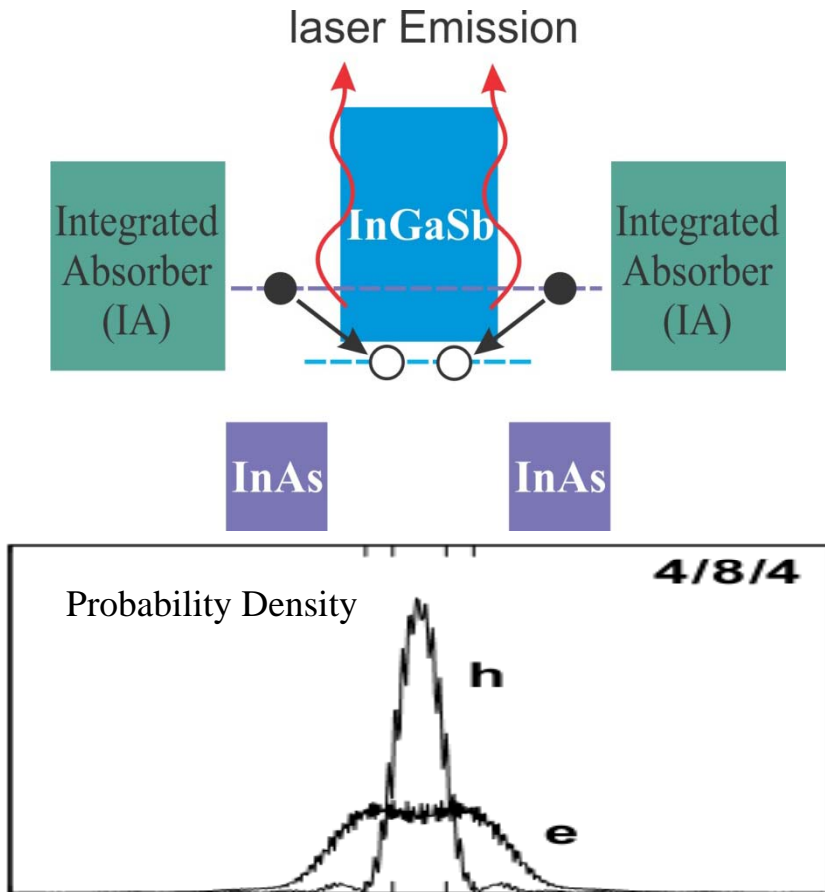
- Applications of Mid-IR Lasers
- Introduction to GaSb Type-II Mid-IR OPSL
- Our approach to achieve tunable DFB laser
- Preliminary experimental results
- Summary

# Applications of Mid-IR Lasers

- Tunable Laser Diode Absorption Spectroscopy (TLDas)
  - Remote chemical/trace gases sensing:  $\text{CH}_4$ ,  $\text{HCl}$ ,  $\text{NH}_3$ ,  $\text{CO}$ ,  $\text{NO}$ ,  $\text{NO}_2$ ...
  - Atmospheric pollution monitoring/leak detection
  - Chemical process control
  - Defense application: chemical warfare agent detection
- IR illumination and range finder
- Infrared countermeasures



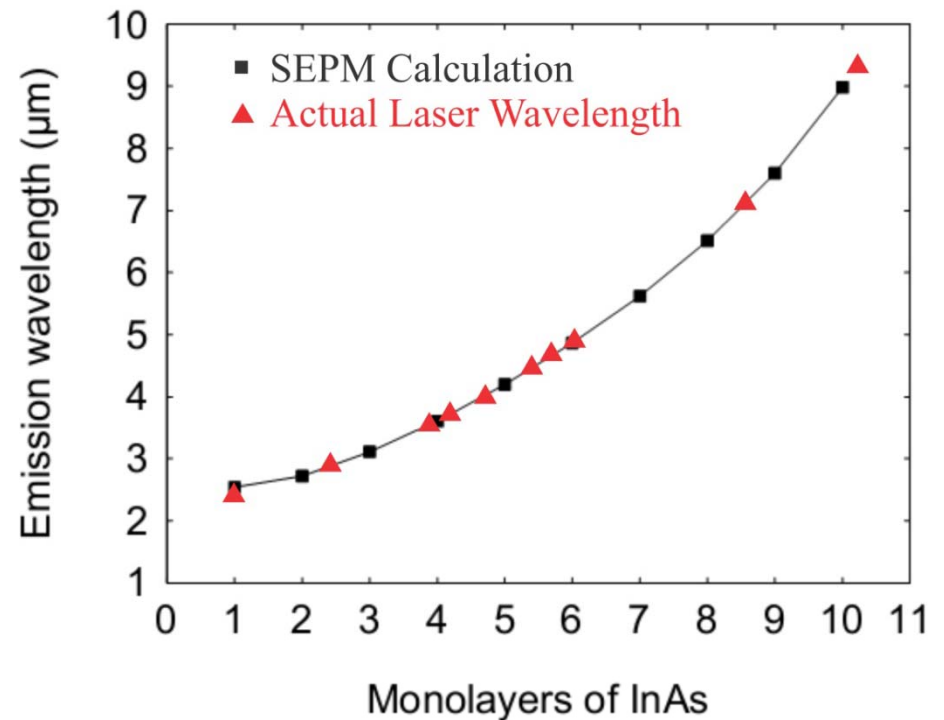
# Introduction to GaSb Type-II Mid-IR OPSL



Meyer et al., APL 67, 1995

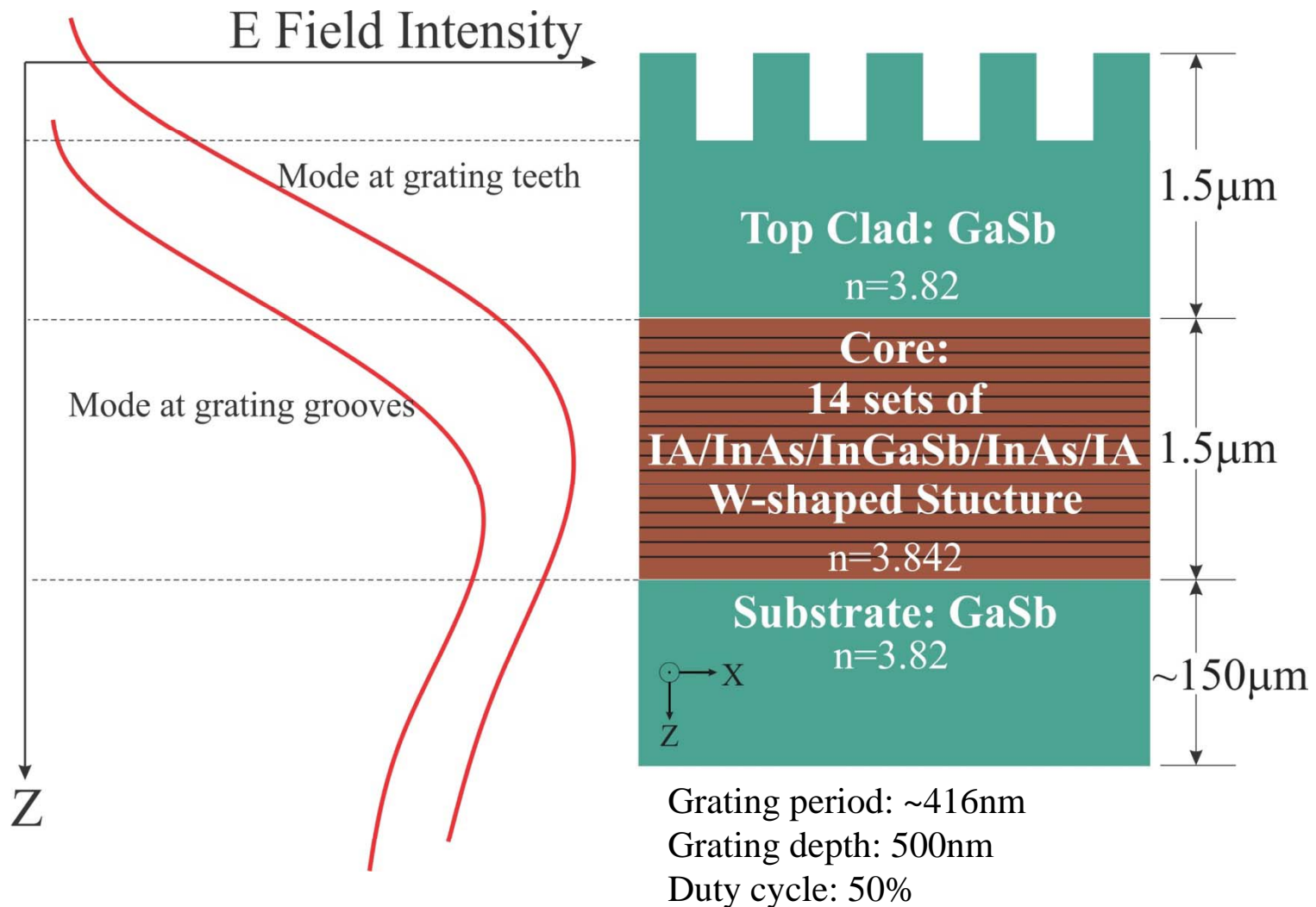
Goyal et al., Proc. LEOS 2000

Lasers span 2.3 – 9.5  $\mu\text{m}$  wavelengths



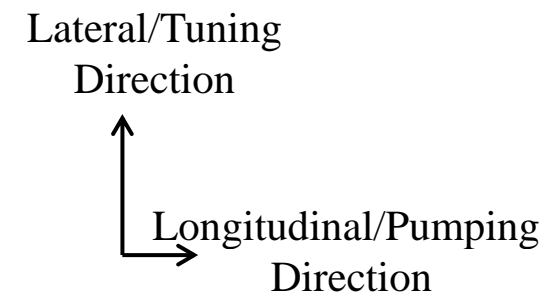
*Kaspi et al.*, Mid-infrared Semiconductor Optoelectronics, Springer

# Slab Waveguide Structure and Mode Distribution



# Our Approach to Tunable DFB Laser

- Chirped grating in top clad of the slab waveguide structure- index coupled DFB laser
- Optically pumped, with flexibility of varying pumping angle/lateral position- gain guided in lateral direction
- Laterally shift pumping stripe at different positions; grating of different periods select different lasing wavelengths to achieve tuning.





# Chirped Grating Period

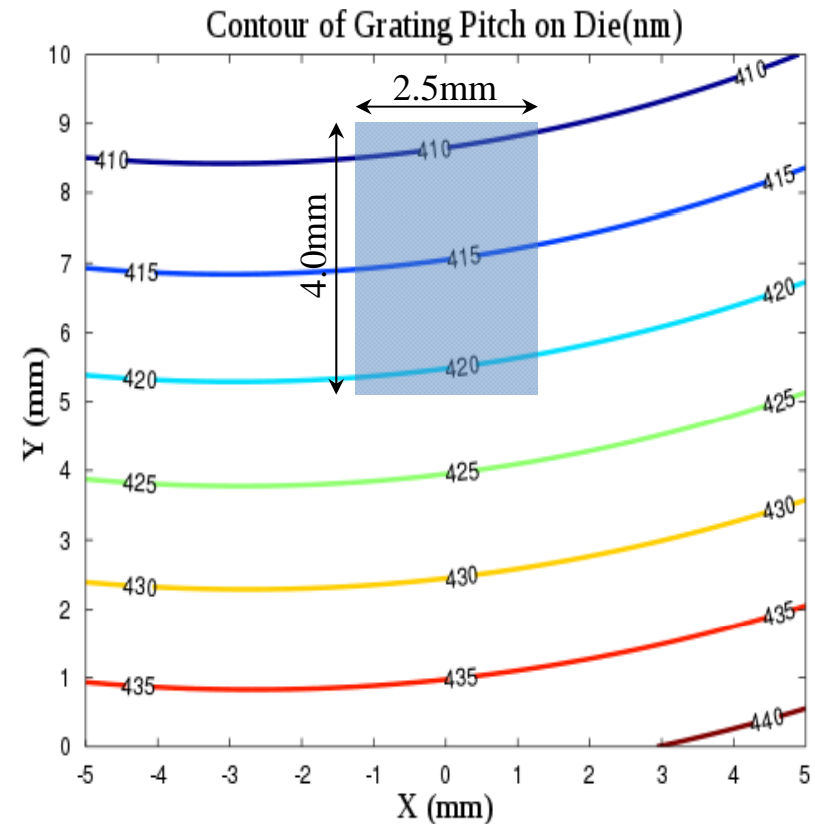
**Grating period:**  $\alpha=6^\circ, \beta=45^\circ$

$$\Lambda = \lambda \cdot \left[ \frac{(u+L)^2 + A - \cos^2 \beta \cdot (c_z - D)^2}{(u+L)^2 + A} + \frac{(u-L)^2 + A - \cos^2 \beta \cdot (c_z - D)^2}{(u-L)^2 + A} - 2 \frac{u^2 - L^2 + A - \cos^2 \beta \cdot (c_z - D)^2}{\sqrt{(u+L)^2 + A} \sqrt{(u-L)^2 + A}} \right]^{-1/2}$$

$$A = v^2 \cos^2 \beta + (v \sin \beta + c_z - D)^2$$

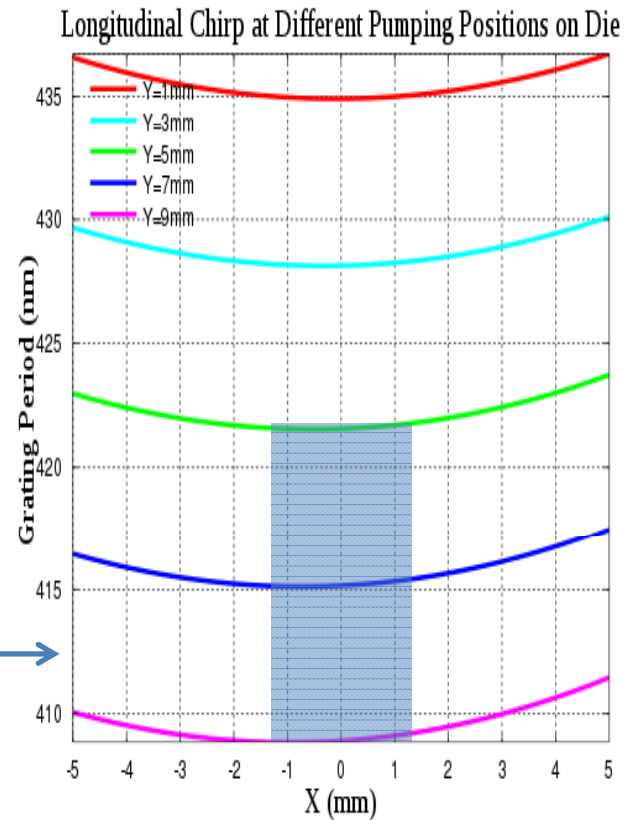
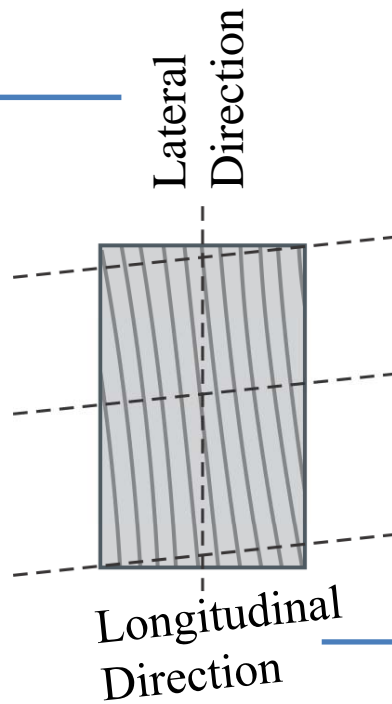
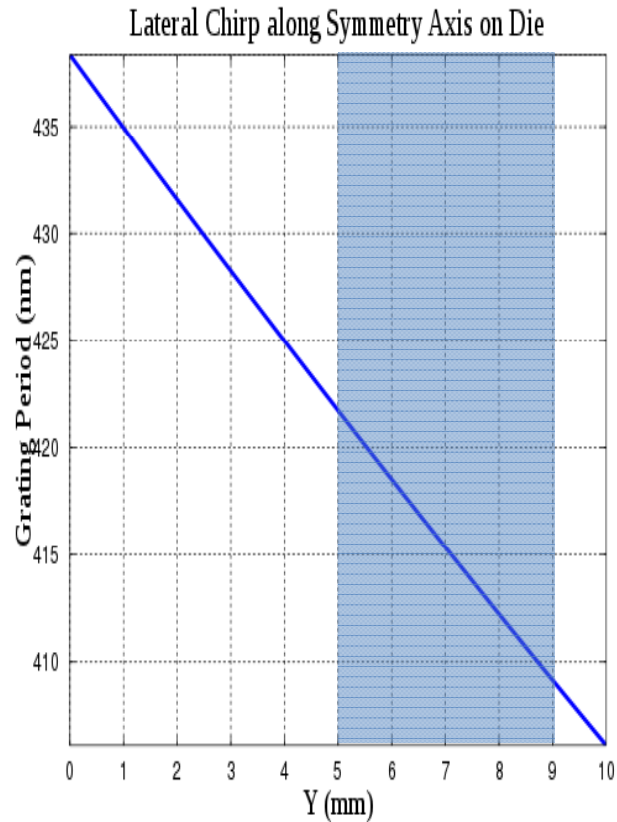
$$u = x \cdot \cos \alpha + y \cdot \sin \alpha;$$

$$v = -x \cdot \sin \alpha + y \cdot \cos \alpha$$



Blue Zone: DFB Device Area

# Chirp of Grating



Blue Zone: DFB Device Area

**4×2.5mm Device:**

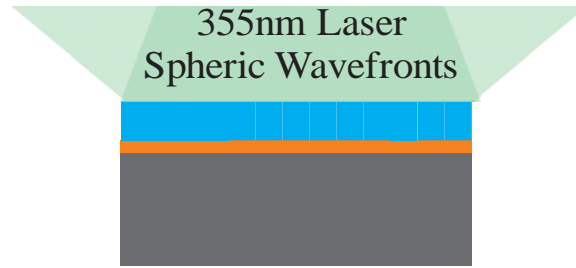
Lateral Chirp along device symmetry axis: **3.05%** , grating period  $\subset [409.2, 421.7]$ nm

Longitudinal Chirp along pump stripe: **0.053%-0.086%**

# Fabrication



PR and ARC Coating

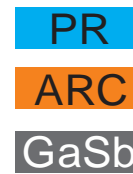


355nm Laser  
Spheric Wavefronts

Chirped Grating  
Exposure by IL



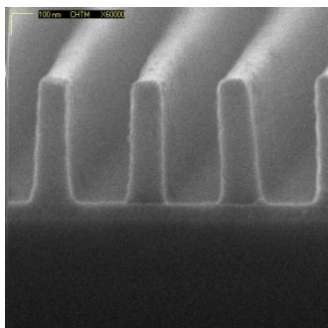
Grating Pattern  
Development



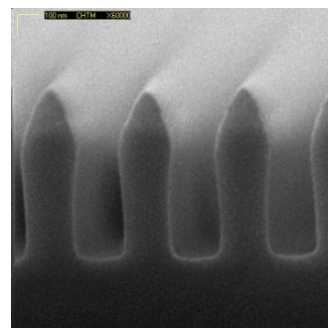
Pattern Transfer  
into Top Clad



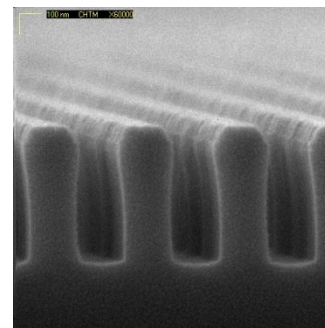
Residual PR and  
ARC Removal



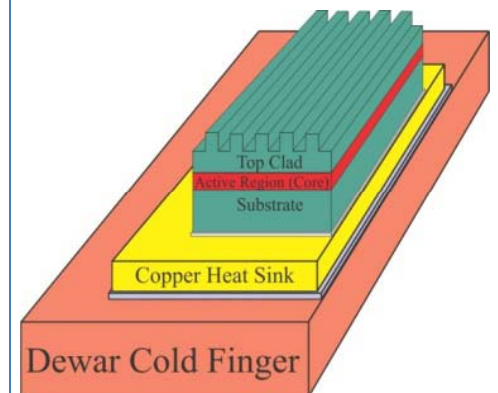
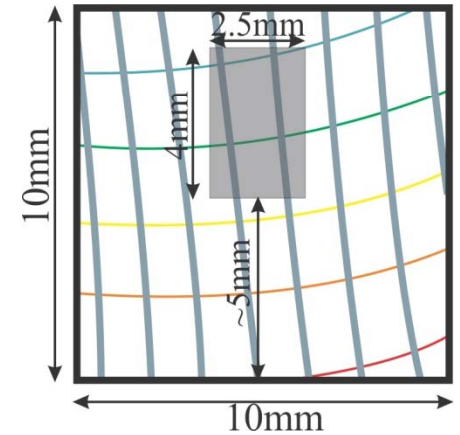
PR Pattern



ICP Etch

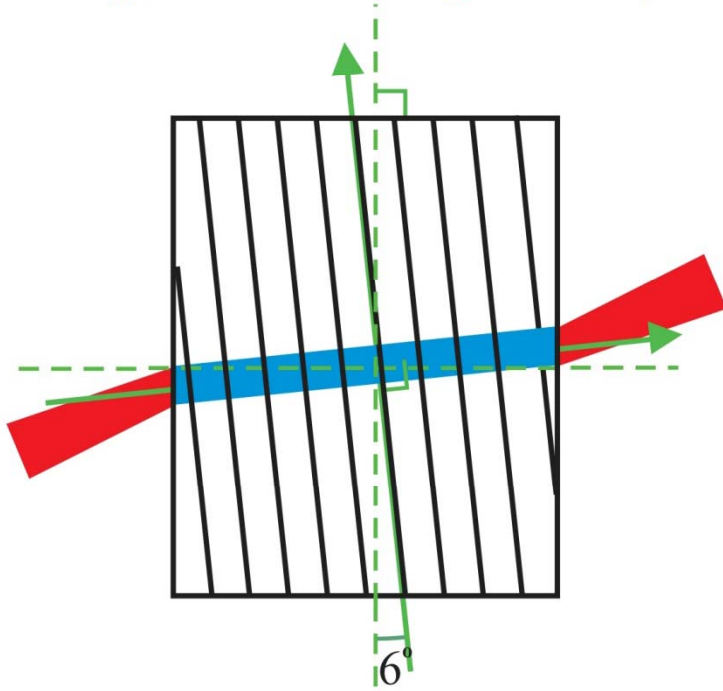


ARC Removal



# Pumping Geometry

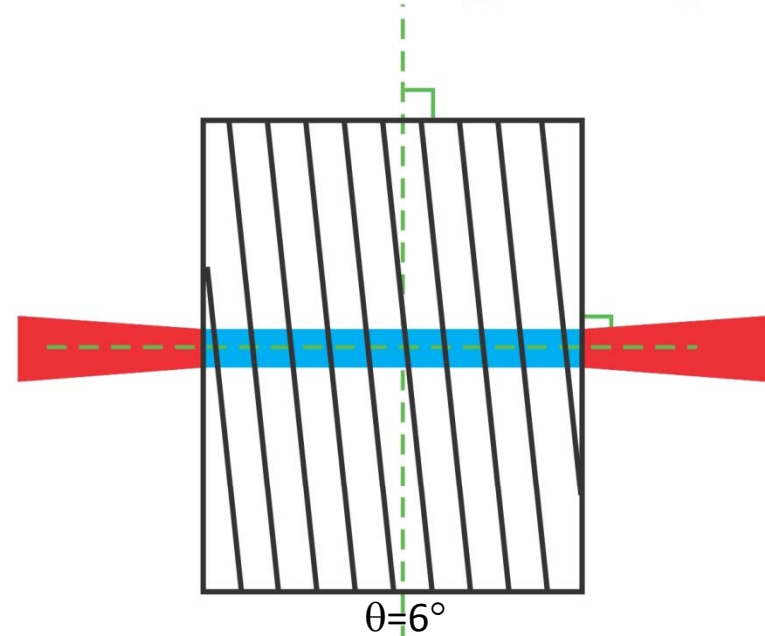
## Grating Normal Configuration(GNC)



$$\lambda_{DFB} = 2n_{eff}\Lambda_{grating}$$

Preferred because of efficient suppression of F-P modes from facet reflection.

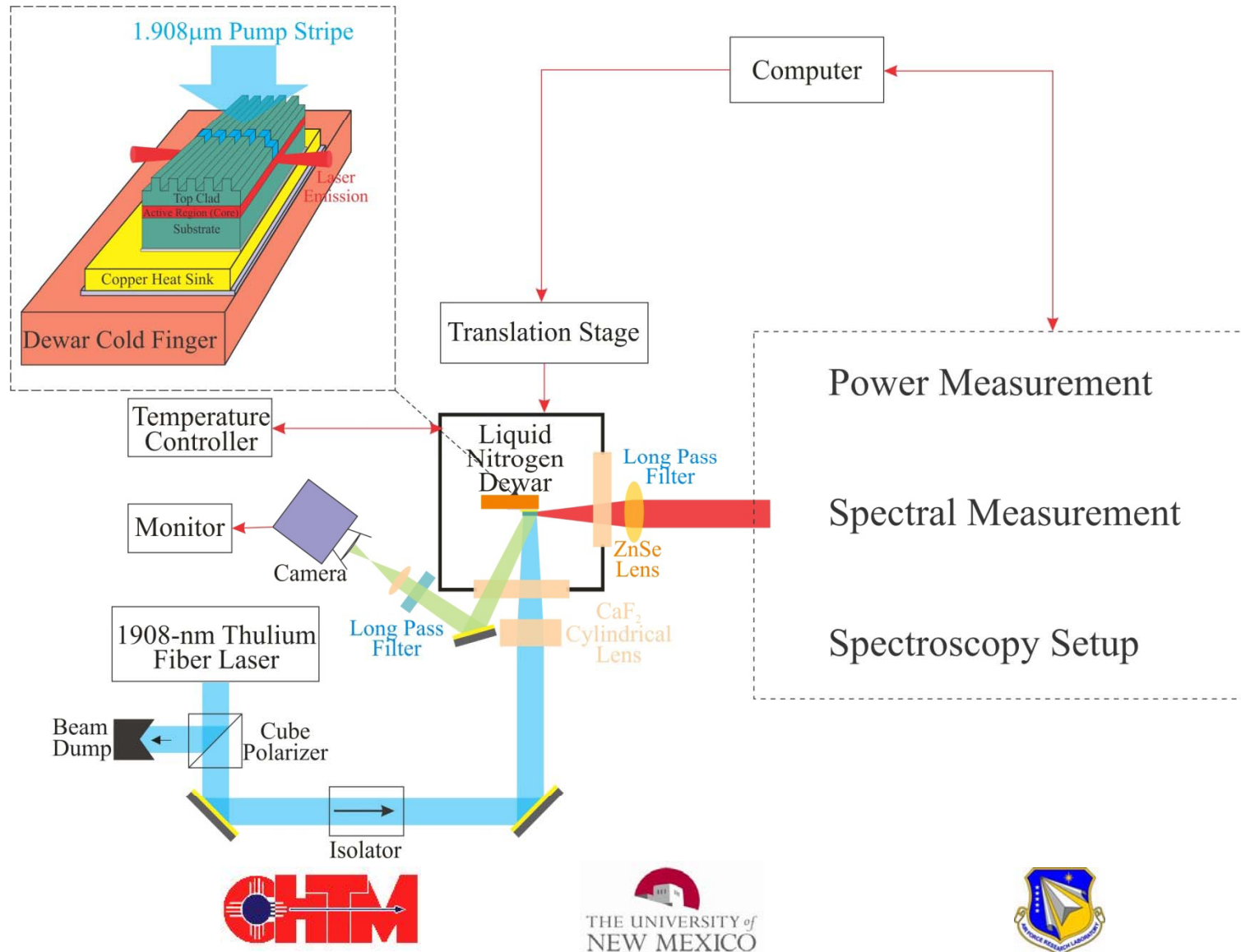
## Facet Normal Configuration(FNC)



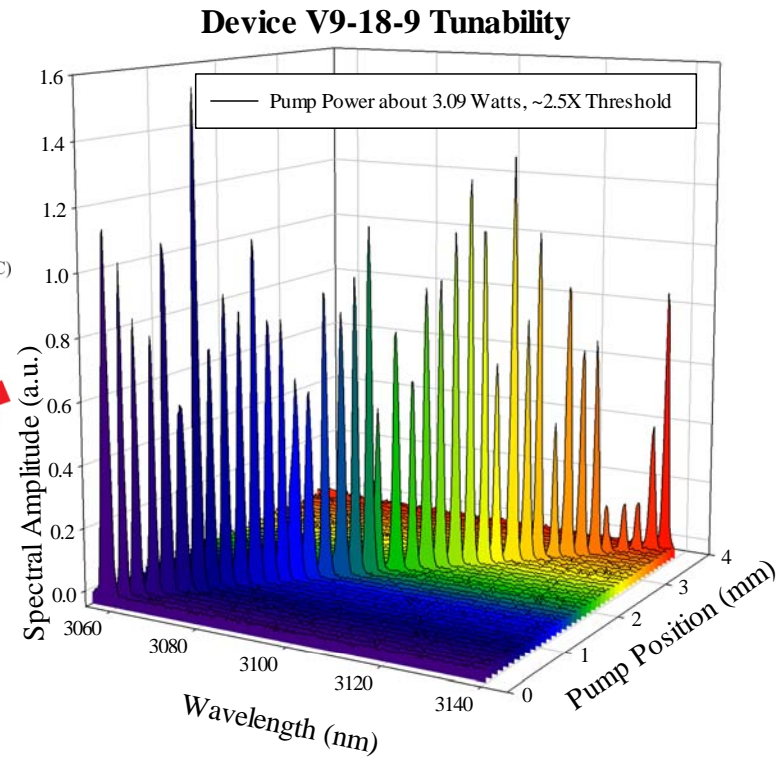
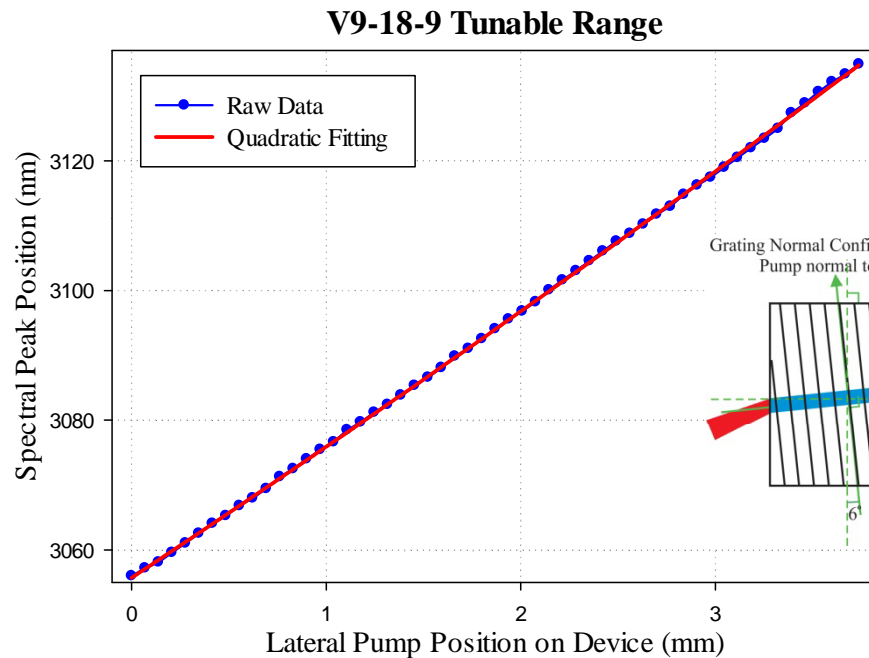
$$\lambda_{\alpha DFB} = 2n_{eff}\Lambda_{grating} \cos(\theta)$$

Take advantage of facet reflection  
Single F-P mode operation at fairly low pump power.

# Experimental Setup

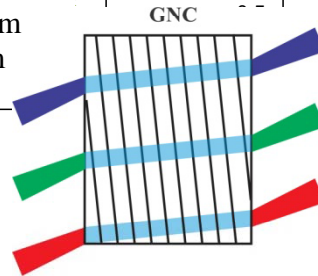
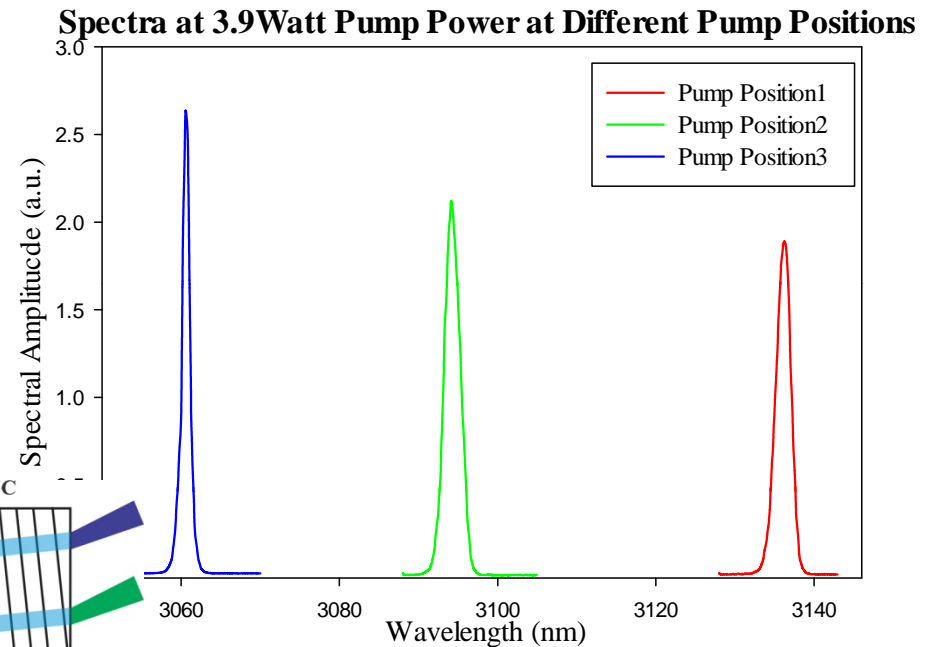
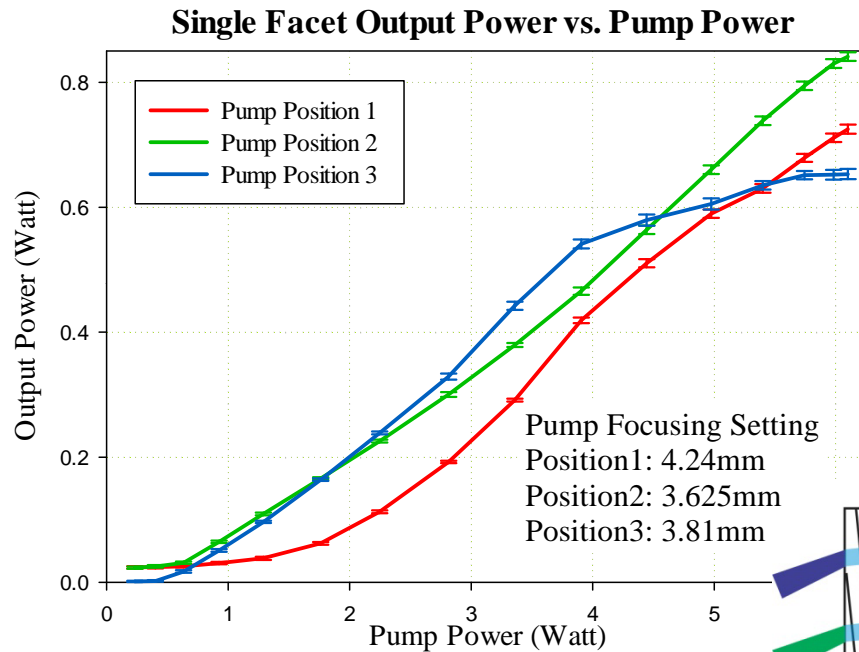


# Tunability Measurement Results



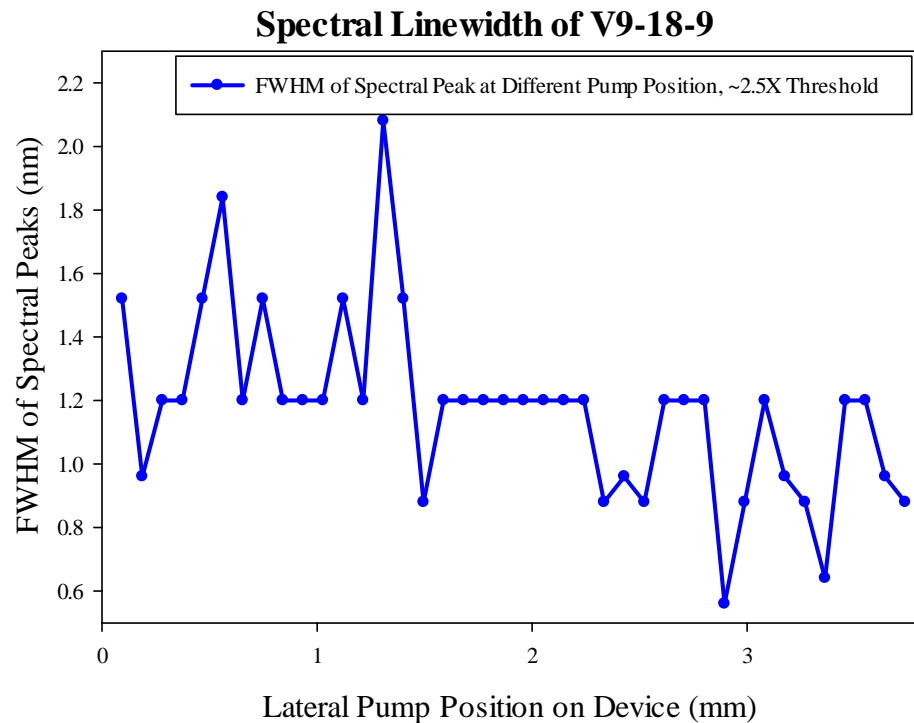
- Continuous tunable range of about **80nm, 3056-3136nm**.
- Single mode(DFB mode) operation across the whole tunable range

# Output Power Measurement



- Achieved over **820mW** single facet output power
- Output power limited by available pump
- Single mode (DFB mode) operation across the whole pump power range

# Spectral Linewidth Measurement



Major factors impacting linewidth:

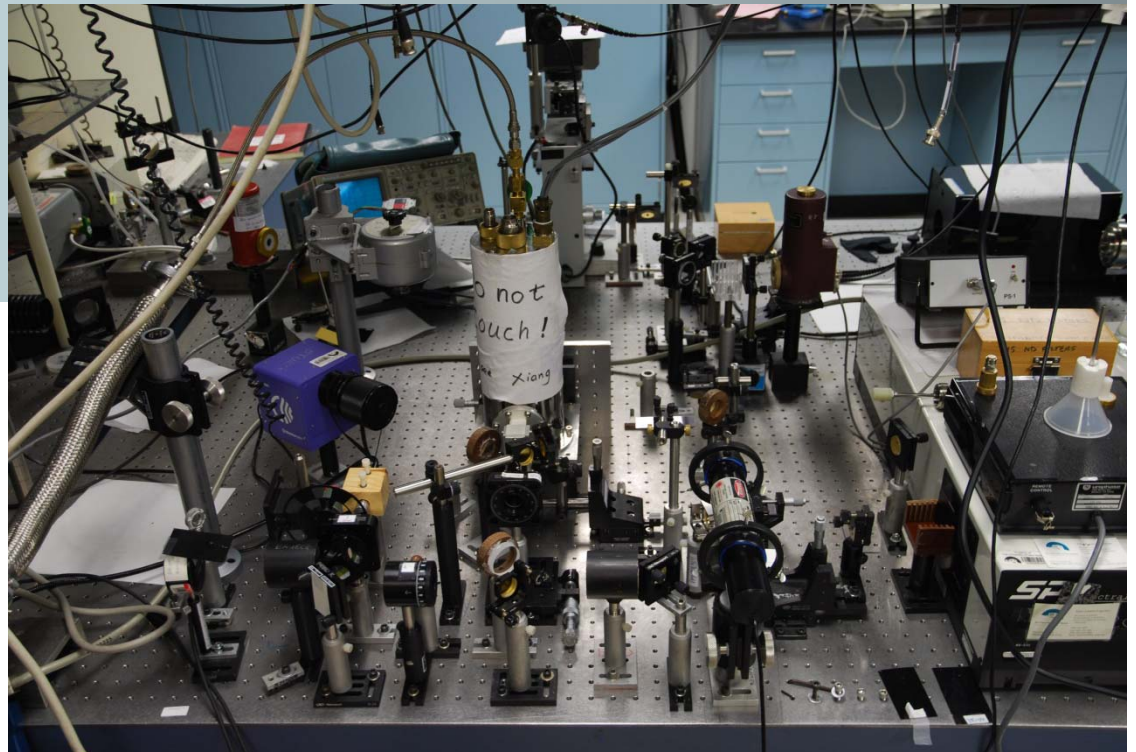
- Longitudinal chirp
- Pump stripe sees lateral chirp
- Linewidth enhancement factor from gain medium

- Typical linewidth: **1.2nm@~2.5×Threshold**, Confirmed by monochromator and F-P interferometer
- Spectral linewidth still wide for low pressure spectroscopy application

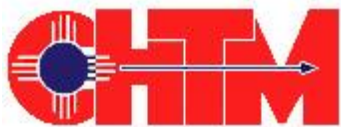
# Summary

- **80nm** tunable range in CW single longitudinal mode operation
- **820mW @ 80K** of single facet output power, limited by available pump
- Typical spectral linewidth of **1.2nm @ 2.5×threshold**
- Optically pumped type-II tunable DFB laser is an excellent high-power widely-tunable single-longitudinal-mode light source for atmospheric pressure spectroscopic applications.
- Novel wavelength tuning method, could be applied to different types of lasers.

**Thank You !  
And  
Questions?**



5/21/2012



17

## Attachment D:

### Non proprietary summary of invention disclosure

Project Title Widely Tunable Optically Pumped Mid-IR DFB Laser

Track Code 2012-102

#### Short Description

Researchers at the University of New Mexico have expanded upon the use of chirped grating systems to allow for the formation of a high-power, optically-pumped, tunable mid-IR laser.

#### Abstract

Chirped gratings are fabricated on the top surfaces of the target substrate, in a longitudinal orientation by translating the pump region up and down to tune the appropriate wavelengths that will be reflected/ transmitted. This form of grating allows for tuning over a wider spectrum. The grating underlying this innovation is achieved through the use of interferometric lithography (IL), where the intensity variation achieved at the point of intersection of two coherent light beams can be used to form grating patterns on a photoresist film, and by controlling the wavefront using a lens system, chirped versus uniform grating can be realized. Once the procedures to finish creation of the distributed feedback (DFB) laser have been completed, the end product is able to operate stably with successful suppression of F-P nodes, and provide continuous tuning over extended wavelength ranges in an extremely robust package.

**DISTRIBUTION LIST  
DTRA-TR-13-62**

**DEPARTMENT OF DEFENSE**

DEFENSE THREAT REDUCTION  
AGENCY  
8725 JOHN J. KINGMAN ROAD  
STOP 6201  
FORT BELVOIR ,VA 22060  
ATTN: J. REED

DEFENSE THREAT REDUCTION  
AGENCY  
8725 JOHN J. KINGMAN ROAD  
STOP 6201  
FORT BELVOIR ,VA 22060  
ATTN: R. KEHLET

DEFENSE TECHNICAL  
INFORMATION CENTER  
8725 JOHN J. KINGMAN ROAD,  
SUITE 0944  
FT. BELVOIR, VA 22060-6201  
ATTN: DTIC/OCA

**DEPARTMENT OF DEFENSE  
CONTRACTORS**

EXELIS, INC.  
1680 TEXAS STREET, SE  
KIRTLAND AFB, NM 87117-5669  
ATTN: DTRIAC

OFFICE OF THE VICE PRESIDENT  
FOR RESEARCH  
UNIVERSITY STRATEGIC  
PARTNERSHIP  
MSC02 1660  
1 UNIVERISITY OF NEW MEXICO  
ALBUQUERQUE, NEW MEXICO  
87131